



**HAL**  
open science

## Proinflammatory Signature of the Dysfunctional Endothelium in Pulmonary Hypertension. Role of the Macrophage Migration Inhibitory Factor/CD74 Complex

Morane Le Hiress, Ly Tu, Nicolas Ricard, Carole Phan, Raphaël Thuillet, Elie Fadel, Peter Dorfmueller, David Montani, Frances S de Man, Marc Humbert, et al.

### ► To cite this version:

Morane Le Hiress, Ly Tu, Nicolas Ricard, Carole Phan, Raphaël Thuillet, et al.. Proinflammatory Signature of the Dysfunctional Endothelium in Pulmonary Hypertension. Role of the Macrophage Migration Inhibitory Factor/CD74 Complex. *American Journal of Respiratory and Critical Care Medicine*, 2015, 192 (8), pp.983-997. 10.1164/rccm.201402-0322OC . inserm-02579320

**HAL Id: inserm-02579320**

**<https://inserm.hal.science/inserm-02579320>**

Submitted on 19 May 2020

**HAL** is a multi-disciplinary open access archive for the deposit and dissemination of scientific research documents, whether they are published or not. The documents may come from teaching and research institutions in France or abroad, or from public or private research centers.

L'archive ouverte pluridisciplinaire **HAL**, est destinée au dépôt et à la diffusion de documents scientifiques de niveau recherche, publiés ou non, émanant des établissements d'enseignement et de recherche français ou étrangers, des laboratoires publics ou privés.

# Pro-inflammatory Signature of The Dysfunctional Endothelium In Pulmonary Hypertension: Role of MIF/CD74 complex

Morane Le Hiress<sup>1,2</sup>, Ly Tu<sup>1,2</sup>, Nicolas Ricard<sup>1,2</sup>, Carole Phan<sup>1,2</sup>, Raphaël Thuillet<sup>1,2</sup>, Elie Fadel<sup>1,2</sup>, Peter Dorfmüller<sup>1,2</sup>, David Montani<sup>1,2,3</sup>, Frances de Man<sup>4</sup>, Marc Humbert<sup>1,2,3</sup>, Alice Huertas<sup>1,2,3</sup>, Christophe Guignabert<sup>1,2,#</sup>

<sup>1</sup> INSERM UMR\_S 999, LabEx LERMIT, Centre Chirurgical Marie Lannelongue, Le Plessis-Robinson, France; <sup>2</sup> Univ Paris-Sud, School of medicine, Kremlin-Bicêtre, France; <sup>3</sup> AP-HP, Service de Pneumologie, Centre de Référence de l'Hypertension Pulmonaire Sévère, DHU Thorax Innovation, Hôpital de Bicêtre, France; <sup>4</sup> Dept. of Pulmonology, VU University Medical Center/Institute of Cardiovascular Research, Amsterdam, The Netherlands.

**#Address correspondence to:** Christophe Guignabert, Ph.D; INSERM UMR\_S 999; Centre Chirurgical Marie Lannelongue; 133, Avenue de la Résistance; 92350 Le Plessis-Robinson, France. Tel: +33 1 40948833; Fax: +33 1 40942522; [christophe.guignabert@inserm.fr](mailto:christophe.guignabert@inserm.fr)

**Authors' contributions:** Conception and design: MLH, LT and CG; Analysis and interpretation: all; Drafting manuscript: LT, MLH, AH, MH, and CG.

**Running title:** Pro-inflammatory endothelial phenotype in PAH

**Funding footnote:** This research was supported by grants from the French National Institute for Health and Medical Research (INSERM) and the French National Agency for Research: grant no. ANR\_12\_JSV1\_0004\_01.

**Manuscript Word Count:** 3490

"This article has an online data supplement, which is accessible from this issue's table of content online at [www.atsjournals.org](http://www.atsjournals.org)"

## Scientific knowledge on the subject

- Inflammatory processes are prominent in various types of human and experimental pulmonary hypertension (PH) and are increasingly recognized as major pathogenic components of pulmonary vascular remodeling.
- CD74 (invariant chain, li) demonstrates high-affinity binding to the pro-inflammatory cytokine macrophage migration-inhibitory factor (MIF), and the MIF homologue D-dopachrome tautomerase (DDT).
- This ligand/receptor complex initiates survival pathways and cell proliferation, triggers the synthesis/ secretion of major pro-inflammatory factors and cell adhesion molecules.

## What this study adds to the field

- Dysfunctional pulmonary endothelial cells (ECs) from idiopathic PH patients exhibit a steady state pro-inflammatory phenotype *in situ* and *in vitro*.
- The pro-inflammatory cytokine MIF and the endothelial receptor CD74 are increased in human and experimental PH and contribute to the endothelial pro-inflammatory phenotype and to an exaggerated recruitment of PBMCs to pulmonary PAH ECs.
- Daily curative treatment of rats with the MIF antagonist ISO-1 or with anti-CD74 neutralizing antibodies started 2 weeks after a subcutaneous monocrotaline injection substantially attenuates the abnormal pulmonary endothelial pro-inflammatory phenotype and partially regresses established PH.

These findings offer new insight into the importance of MIF/CD74 complex in PH. We provide the first *in situ* and *in vitro* demonstration that pulmonary ECs from idiopathic PH patients exhibit a steady state pro-inflammatory phenotype. Furthermore, our findings underscore for the first time the critical role of MIF and CD74 in this process. These results strongly support that MIF and its signaling through CD74 are key players at the crossroad of inflammation, cancer-like phenotype and endothelial dysfunction in PAH pathogenesis.

## **ABSTRACT**

**Rationale:** Inflammation and endothelial dysfunction are considered two primary instigators of pulmonary arterial hypertension (PAH). CD74 is a receptor for the pro-inflammatory cytokine macrophage migration-inhibitory factor (MIF). This ligand/receptor complex initiates survival pathways and cell proliferation, triggers the synthesis/secretion of major pro-inflammatory factors and cell adhesion molecules.

**Objectives:** We hypothesized that MIF/CD74 signaling pathway is over-expressed in idiopathic PAH (iPAH) and contributes to a pro-inflammatory endothelial cell (EC) phenotype.

**Measurements and Main Results:** In human lung tissues, ICAM-1, VCAM-1, and E-selectin expressions are markedly up-regulated in endothelium of distal iPAH pulmonary arteries. Circulating MIF levels are increased in serum of PAH patients as compared to controls and T-cell lymphocytes represent a source of this overabundance. In addition, CD74 is highly expressed in the endothelium of muscularized pulmonary arterioles and in cultured pulmonary ECs from iPAH, contributing to an exaggerated recruitment of peripheral blood mononuclear cells (PBMCs) to pulmonary iPAH ECs. Finally, we found that curative treatments with the MIF antagonist ISO-1 or anti-CD74 neutralizing antibodies partially reverse development of pulmonary hypertension in rats and substantially reduced inflammatory cell infiltration.

**Conclusions:** We report here that CD74 and MIF are markedly increased and activated in iPAH patients, contributing to the abnormal pro-inflammatory phenotype of pulmonary ECs in iPAH.

***Word count:*** 206 words

***Keywords:*** pulmonary hypertension • endothelial dysfunction • macrophage migration inhibitory factor • CD74 signaling pathway • adhesion molecules

## INTRODUCTION

Pulmonary arterial hypertension (PAH) is a rare and severe disease characterized by vascular proliferation and remodeling of the small pulmonary arteries leading to a progressive increase in pulmonary vascular resistance and ultimately to right ventricular failure and death. PAH constitutes a heterogeneous group of clinical entities sharing similar physiopathological mechanisms, whereas idiopathic PAH (iPAH) corresponds to sporadic disease in which there is neither a family history of PAH nor an identified risk factor (1, 2). Although the exact mechanisms leading to the onset and progression of PAH are still largely unclear, a complex interplay between pulmonary endothelial dysfunction and inflammation is strongly suspected to influence the development of the disease (3). However, the underlying mechanisms linking characteristics of dysfunctional pulmonary endothelium and the development of PAH have not been fully elucidated.

CD74 (invariant chain, Ii) is a non-polymorphic transmembrane glycoprotein that exists in different isoforms and plays a major role in regulating the trafficking of major histocompatibility complex (MHC) class II proteins in antigen-presenting cells (4). However, CD74 can also be expressed in the absence of the MHC class II protein (2-5%) and has recently been reported to be a high-affinity binding protein for the pro-inflammatory cytokine macrophage migration inhibitory factor (MIF), providing evidence for a role in signal transduction pathways (4, 5). The lung is a major source of MIF, which is released upon stimulation by stress, endotoxins, inflammatory and immune stimuli and plays a pivotal upstream role in the inflammatory cascade by promoting the release of other inflammatory cytokines (tumor necrosis factor (TNF)- $\alpha$ , interleukin (IL)-1, IL-6, IL-8, IL-12, interferon- $\gamma$ ...) (6-8). Stimulation of CD74 initiates a signaling cascade through the sustained and transient activation of the mitogen-activated protein kinases (MAPKs), extracellular signal-regulated kinase (ERK)1 and ERK2, protein kinase B (Akt) and nuclear factor (NF)- $\kappa$ B, leading to leukocytic integrin activation, cell proliferation, and survival and induction of pro-inflammatory gene expression (5, 7, 9-13). CD74 is known to be present in limited amounts in endothelial

cells (ECs) in physiological conditions and overexpressed in certain physiopathological conditions (26). However, the endothelial MIF/CD74 expression and activity patterns and its contribution to PAH progression remain unanswered questions. Therefore, we hypothesized that endothelial CD74 could be a key molecule at the crossroad of inflammation and pulmonary endothelial dysfunction in PAH, contributing to the endothelial pro-inflammatory phenotype. We investigated: 1) the endothelial pro-inflammatory activation state in iPAH *in situ* and *in vitro*; 2) the MIF levels in the serum of iPAH patients and controls; 3) the *in situ* CD74 protein expression within walls of iPAH and control pulmonary arteries; 4) whether or not intrinsic abnormalities in the endothelial CD74 signaling pathway are a characteristic of pulmonary ECs (P-ECs) from iPAH patients; 5) whether or not the abnormal CD74 activation in P-ECs can contribute to the pulmonary endothelial pro-inflammatory phenotype, through modulation of the expression of proteins involved in leukocyte recruitment or adhesion; 6) the MIF levels in the serum and the CD74 protein expression in two rodent models of pulmonary hypertension (PH); 7) the efficacies of curative treatments with either the MIF antagonist ISO-1 or anti-CD74 neutralizing antibodies on the aberrant pro-inflammatory endothelial phenotype *in vitro* and *in vivo* and on the progression of monocrotaline (MCT)-induced PH.

## **METHODS**

### **Study population**

For the *in vitro* and *in situ* studies, we used lung specimens obtained during lung transplantation in patients with iPAH or heritable PAH (hPAH) and during lobectomy or pneumonectomy for localized lung cancer in control subjects (Supplemental Table 1 for clinical data). The lung specimens from the controls were collected at a distance from the tumor *foci*. This study was approved by the local ethics committee (CPP Ile-de-France VII, Le Kremlin-Bicêtre, France). All patients gave informed consent before the study.

## **Isolation, culture and functional analyses of human pulmonary endothelial cells (P-ECs)**

Human P-ECs were isolated and cultured as previously described (14-19). The isolated P-ECs were strongly positive for acetylated low-density lipoprotein coupled to Alexa 488 (Alexa488-Ac-LDL), von Willebrand factor (vWF), CD31, and for Ulex europaeus agglutinin-1 (UEA-1) and negative for alpha-smooth muscle actin ( $\alpha$ -SMA) (Supplemental Fig S1). To suppress CD74 expression, P-ECs were transfected using lipofectamine RNAiMAX with 100 nM of CD74 siRNA or with a scrambled sequence (Invitrogen, Cergy-Pontoise, France). To overexpress CD74, P-ECs were transfected using lipofectamine 2000 with 1  $\mu$ g of a full-length human CD74 (p35 isoform) construct in the pcDNA 3.1/v5-His/CD74 plasmid (20) kindly provided by Pr. Richard Bucala (Yale University School of Medicine, New Haven, CT, USA) or with 1  $\mu$ g of pcDNA 3.1/v5-His/LacZ plasmid. The cells were studied within 3 days after transfection. Suppression or overexpression of CD74 levels was documented 72 hours after transfection. Human peripheral blood mononuclear cells (PBMCs) were isolated from whole blood of control patients using Ficoll density gradient centrifugation and labeled with dichlorofluorescein (Molecular Probes, Cergy-Pontoise, France). PBMCs ( $1 \times 10^6$  cells/ 6-well-plate) were added for 3h to confluent iPAH or control EC monolayers previously labeled with CellTracker<sup>TM</sup> probes (Molecular probes) and preincubated or not for 24 h with recombinant human MIF (100 ng/ml, Raybiotech, Le Perray en Yvelines, France). Non-adherent PBMCs were then removed and nuclei labeled with DAPI. The total number of adherent PBMCs was determined in 3 randomly high-powered fields/ well acquired with a fluorescence microscope Nikon Eclipse 80i and NIS-Elements BR 2.30 software. Migration of PBMCs was assayed in 24-well cell-culture chambers using inserts with 3- $\mu$ m pore membranes as previously described (18, 19). Briefly, conditioned media with similar pH from confluent control and iPAH P-EC monolayers, collected at 24 hours and used pure, were added to the lower compartment of a modified Boyden chamber, while freshly human PBMCs isolated from whole blood of control patients were placed to the upper compartment for 4 hours. The

numbers of migrating PBMCs that migrated to the lower compartment were counted by flow cytometry after Hoechst 33342 staining.

### **Total RNA isolation and *real-time* quantitative PCR**

The mRNA expression of IL-1 $\alpha$ , IL-1 $\beta$ , IL-6, IL-8, IL-12, monocyte chemoattractant protein-1 (MCP)-1, intercellular adhesion molecule (ICAM)-1, vascular cell adhesion molecule (VCAM)-1, P-selectin and E-selectin was measured by *real-time* quantitative PCR as previously described (15, 19, 21). Relative quantification was calculated by normalizing the Ct (threshold cycle) of the gene of interest to the Ct of 18S in the same sample, according to the comparative CT method ( $\Delta\Delta$ CT method).

### **Flow cytometry analyses**

After blood samples withdrawal, PBMCs from iPAH patients and controls were obtained by Ficoll density gradient centrifugation using standard UNI-SEP+ system (Eurobio, Courtaboeuf, France). The cells were carefully washed with PBS and resuspended in a staining buffer containing 5% of BSA. The cells were fixed then fluorescently labeled with the following antibodies under permeabilized conditions (IntraPrep, following manufacturer's instructions, Beckman Coulter, Nyon, Switzerland): fluorophore conjugated monoclonal anti-CD19, monoclonal anti-CD3, monoclonal anti-CD14 (Becton Dickinson, Le Pont de Claix, France), and polyclonal anti-MIF (BIOSS, Montluçon, France). Flow cytometry gating conditions and the mean fluorescence intensity (MFI) were set and normalized, respectively, against isotype- and fluorophore-matched non-immune immunoglobulins (IgGs). Flow cytometry data were acquired with a flow cytometer (MACSQuant, Miltenyi Biotec, Paris, France) and analyzed by FlowJo software program (Tree Star, Inc).

### **Western blot, ELISA, and Immunostaining**

Cells/tissues were homogenized and sonicated in PBS containing protease and phosphatase inhibitors and 30  $\mu$ g of protein was used to detect CD74 (Santa Cruz, Dallas, TX, USA) and  $\beta$ -actin (Sigma-Aldrich, Saint-Quentin Fallavier, France) as previously described (19).

Concentrations of IL-6, and MCP-1 in serum were evaluated using Quantikine (R&D Systems, Lille, France) according to the manufacturer instructions. Immunohistochemistry and immunocytofluorescent staining for ICAM-1 (Santa Cruz), VCAM-1 (Abcam, Paris, France), E-selectin,  $\alpha$ -SMA (Santa Cruz), CD3, CD45 (BD Pharmingen, Le Pont de Claix, France) and CD68 (Santa Cruz) were performed as previously described (15, 19, 22). Images were taken using LSM700 confocal microscope (Zeiss, Marly Le Roi, France). Quantifications of the mean fluorescence intensity (MFI) for endothelial ICAM-1, VCAM-1 and E-selectin were performed in vWF<sup>+</sup> cells of 5-10 remodeled vessels per subjects (n=8 for each groups) using Zen software (Zeiss, Marly Le Roi, France) or in P-ECs using a 60 x objective viewing fields using ImageJ (National Institutes of Health, Bethesda, MD, USA).

### **Rodent models of pulmonary hypertension**

Animal studies were approved by the administrative panel on animal care at the Univ. Paris-Sud, Le Plessis-Robinson, France. Young male Wistar rats (100 g, Janvier Labs, Saint Berthevin, France) were either studied 3 weeks after a single subcutaneous injection of monocrotaline (MCT) (60 mg/kg; Sigma-Aldrich) or vehicle (21), or 3 weeks after chronic exposure to hypoxia (10% oxygen) or in room air (23). Two weeks after a single subcutaneous injection of MCT, rats were randomly divided into 3 groups and treated for 2 weeks with daily intraperitoneal injections of (S,R)-3-(4-hydroxyphenyl)-4,5-dihydro-5-isoxazole acetic acid methyl ester (ISO-1) (at a dose of 10 or 30mg/kg/day) and vehicle (a 50:50 mix of normal saline and dimethyl sulfoxide (DMSO)). In an additional experiment, MCT-injected rats were randomly divided into 4 groups and treated with 3 intraperitoneal injections of anti-CD74 neutralizing antibodies (Santa Cruz) (15 or 30 $\mu$ g/kg), IgG isotype (Santa Cruz) (30 $\mu$ g/kg) during 1 week. Animals were anesthetized with isoflurane. A polyvinyl catheter was introduced into the right jugular vein and pushed through the right ventricle into the pulmonary artery. Cardiac output in rats was measured using the thermodilution method. After measurement of hemodynamic parameters, the thorax was opened and the left lung immediately removed and frozen. The right lung was fixed in the distended state with

formalin buffer. The right ventricular hypertrophy assessed by the Fulton index [weight ratio of right ventricle (RV) and (left ventricle (LV) + septum)] and the percentage of wall thickness  $[(2 \times \text{medial wall thickness} / \text{external diameter}) \times 100]$  and of muscularized vessels were determined as previously described (15).

### **Cardiac fibrosis analyses**

Heart from MCT-injected rats or control rats were deparaffinized, and stained for collagen using Picrosirius red staining. Three randomly selected fields from transversally sectioned tissue were used. Fibrosis areas of both right and left ventricle myocardium were quantified using ImageJ software and expressed as collagen area fraction.

### **Statistical Analyses**

The data are expressed as mean  $\pm$  SEM. Statistical significance was tested using the nonparametric Mann-Whitney test or two-way ANOVA with Bonferroni post hoc tests. Significant difference was assumed at a p value of  $< 0.05$ .

## **RESULTS**

### **Pulmonary ECs from iPAH patients exhibit a steady state pro-inflammatory phenotype**

To determine whether the pulmonary endothelium in PAH is characterized by a transition from a quiescent state (without adhesion capacity) to an activated state with adhesive capacity, confocal microscopic analyses and double labeling with either ICAM-1, VCAM-1 and E-selectin were used to investigate the adhesion molecule expression on P-ECs in lung specimens from 8 patients with iPAH and 8 control subjects (Supplemental Table 1). We found strong staining for these adhesion molecules in paraffin-embedded lungs of patients with iPAH when compared with controls (Figure 1). Interestingly, we found strong ICAM-1 (Figure 1A, 1D and Supplemental Fig S2), VCAM-1 (Figure 1B, 1D and Supplemental Fig S2), and E-selectin (Figure 1C, 1D and Supplemental Fig S2) expressions within the

endothelium of distal pulmonary arteries from patients with iPAH as compared with a weak staining within the endothelium of control specimens.

Consistent with these *in situ* observations, we found that freshly isolated human P-ECs from iPAH patients exhibited also a marked pro-inflammatory transcriptional signature. Primary early (< 3) passage cultures of human ECs isolated from lung tissues obtained from iPAH patients displayed higher expressions of IL-1 $\alpha$ , IL-6, IL-8, IL-12, MCP-1, E-selectin, ICAM-1, P-selectin, and VCAM-1 as compared to control cells (Figure 2A, Supplemental Table 1, and Fig S1). To investigate the functional consequences of these gene expression changes, modified Boyden chamber assays were first used to study the ability of P-ECs from iPAH and controls to attract leukocytes. We noted that the migratory capacity of PBMCs was substantially increased (up to 4-fold) in presence of conditioned media of quiescent cultured human P-ECs from patients with iPAH when compared with conditioned media of control cells (Figure 2B). In addition, we also found that the amount of bound PBMCs on confluent cell monolayers is about 2- to 3-times higher when iPAH ECs were used as compared to control ECs (69 $\pm$ 13 *versus* 35 $\pm$ 11 adherent PBMCs per field in absolute numbers) (Figure 2C).

### **Increased expression patterns of MIF and CD74 in iPAH patients**

A substantial increase in circulating MIF protein levels was observed in the serum of PAH patients compared with controls (147 $\pm$ 14 *versus* 66 $\pm$ 7 ng/mL respectively;  $p < 0.001$ ) (Figure 3A and Supplemental Table 2) [No significant difference was noted between iPAH and hPAH patients ( $p = 0.20$ , NS; Supplemental Fig S3)]. In contrast, circulating protein levels of the MIF homologue D-dopachrome tautomerase (DDT) were similar to levels found in a control population (7.4 $\pm$ 2.2 *versus* 4.6 $\pm$ 1.0 ng/mL respectively; NS) (Figure 3A). Furthermore, we were able to show that T-cell lymphocytes represent a source of this overabundance in iPAH (Figure 3B). In normal tissues, expression of CD74 is limited to B cells, monocytes, macrophages, dendritic cells and epithelial cells of endodermal and mesodermal origin (24, 25). Consistent with this knowledge, our data show several CD74 positive cells in the

pulmonary perivascular area in normal and iPAH lung tissues (Figure 3C and Supplemental Fig S4). In addition, it is also known that CD74 is present in limited amounts in ECs in physiological conditions (24). However, Richard *et al.* recently found an increased endothelial expression of CD74 in human breast cancer (26). Interestingly, we also noted a strong CD74 staining within the endothelium of distal-pulmonary arteries from iPAH patients (arrows), contrasting with a negative or a weak staining for CD74 in control lung tissues (increased by about  $2.1 \pm 0.3$ ,  $p=0.0037$ ;  $n=7-8$  patients) (Figure 3C and Supplemental Fig S4). These *in situ* observations were maintained *in vitro*, with cultured P-ECs from iPAH patients exhibiting increased CD74 protein expression levels as compared to control cells (Figure 3D).

### **MIF/ CD74 is involved in the endothelial pro-inflammatory phenotype and leukocyte recruitment in PAH**

Leukocyte recruitment and arrest are central steps in inflammatory reactions and associated diseases, including PAH (27-29). To study the effect of endothelial CD74 signaling on leukocyte recruitment, subsequent studies were carried out using confluent P-EC monolayers from iPAH and control patients and exogenous MIF. We found that expressions of E-selectin, VCAM-1, ICAM-1 and secretions of endothelial-derived IL-6 and MCP-1 were substantially increased following MIF pretreatment (for 24 hours) in control P-ECs (Figure 4A and B). Consistent with these observations, we found that a pretreatment with MIF for 24 h increased the amount of bound PBMCs on control P-ECs ( $56 \pm 5$  versus  $29 \pm 2$  adherent PBMCs per field in absolute numbers, respectively), a phenomenon that was even more pronounced when iPAH P-ECs were used ( $108 \pm 11$  versus  $48 \pm 5$  adherent PBMCs per field in absolute numbers, respectively) (Figure 4C). Additional experiments were done using control P-ECs expressing different CD74 protein levels. In this complementary approach, we increased the amount of bound PBMCs on confluent EC monolayers overexpressing CD74 ( $69 \pm 2$  versus  $36 \pm 5$  adherent PBMCs per field in absolute numbers, respectively), whereas this amount was lower when decreasing CD74 signaling by RNA interference ( $37 \pm 3$  versus  $26 \pm 6$  adherent PBMCs in absolute numbers) (Figure 4D and Supplemental Fig S5). Finally,

we showed that both ISO-1 and neutralizing antibodies against CD74 are able to decrease the pro-inflammatory signature of P-ECs derived from patients with iPAH (Figure 4E). Of note, since MIF is also known to bind with low nanomolar affinity to CXCR2 and CXCR4, we assessed the role of MIF/CXCR2 and MIF/CXCR4 in the aberrant endothelial pro-inflammatory phenotype and found: no difference in the relative mRNA levels of CXCR2 and CXCR4 in P-ECs from controls and iPAH patients (Supplemental Fig S6A); and no difference in the relative mRNA levels of ICAM-1, VCAM-1 and E-selectin in iPAH P-ECs treated or not with either the selective nonpeptide CXCR2 antagonist SB225002 (5, 25 and 50nM) or the CXCR4 blocking agents AMD3100 (5, 25 and 50  $\mu$ M) for 24h (Supplemental Fig S6B).

### **MIF and CD74 protein levels are increased in two pulmonary hypertension animal models**

To better understand the endothelial MIF/CD74 signaling in the pathogenesis of the disease, we next examined the protein expression pattern of MIF and CD74 in lungs from rodent models of PH. Consistent with findings obtained in human lung tissues, a substantial increase in circulating MIF protein levels was observed in the two well recognized and widely used MCT- and chronic hypoxia-induced PH models (Figure 5A). Since the MCT-induced PH model demonstrated a more significant increase in circulating MIF levels, Western blotting and immunohistochemistry were performed on lung sections of vehicle and MCT-injected rats. Consistent with our findings obtained in human samples, a substantial progressive increase in CD74 protein levels was observed in lungs of MCT-injected rats, starting at Day-14 and reaching a maximal 2- to 3-fold increase after 21 days when compared with their control rats (Figure 5B). In addition, a substantial increase in endothelial CD74 protein levels were also observed *in situ* (Figure 5C and Supplemental Fig S7) and in collagenase-digested lung tissues from MCT-injected rats when compared with their control rats at 21 days (Figure 5D).

### **Efficacy of treatment with the MIF antagonist ISO-1 on the progression of MCT-induced PH and on the abnormal pulmonary endothelial pro-inflammatory phenotype**

Daily treatment with the MIF antagonist ISO-1 started 2 weeks after a subcutaneous MCT injection substantially attenuates the abnormal pulmonary endothelial pro-inflammatory phenotype and regresses established PH (Figure 6). On day 21, in MCT-injected rats treated with vehicle, a marked increase in mean pulmonary arterial pressure (mPAP), RV/(LV+ S) ratio, percentage medial wall thickness, and numbers of muscularized distal pulmonary arteries were found compared with controls (Figure 6A and B). However, we noted that MCT-injected rats receiving ISO-1 at the dose of 30 mg/kg exhibited reduced cardiac output as compared to MCT-injected rats receiving vehicle (Figure 6A). Notably, there was no significant difference in values of mPAP, right ventricular hypertrophy, and cardiac output between control rats treated with either ISO-1 at the doses of 10 - 30 mg/kg or vehicle (Supplemental Fig S8). To investigate the efficacy of ISO-1 treatment on the abnormal pulmonary endothelial pro-inflammatory phenotype, we conducted parallel evaluations of the cell surface expression of cell adhesion molecules on endothelial cells, of circulating IL-6 and MCP-1 levels, and of pulmonary infiltration. On day 21, levels of endothelial ICAM-1, VCAM-1, E-selectin were substantially reduced in lungs of MCT-injected rats treated with ISO-1 when compared to MCT-injected rats treated with vehicle (Figure 6C). In addition, we noted a substantial reduction in circulating levels of IL-6 and MCP-1 in MCT-injected rats treated with the highest dose of ISO-1 (Figure 6D). Consistent with these findings, numbers of CD45-, CD3- and CD68-positive cells were markedly reduced when compared to vehicle-treated rats (Supplemental Fig S9, panel A).

### **Reversal of MCT-induced PH with anti-CD74 neutralizing antibodies**

To further demonstrate that the decrease in pulmonary vascular changes and PH severity obtained with ISO-1 were produced by the decreased endothelial-MIF/CD74 signaling, we have investigated whether selective anti-CD74 neutralizing antibodies reversed PH induced by MCT in rats. In rats treated with anti-CD74 neutralizing antibodies (30) at the dose of 30  $\mu$ g/kg, a marked decrease in mPAP, RV/(LV+ S) ratio, percentage medial wall thickness and distal artery muscularization was observed compared to rats treated with 30  $\mu$ g/kg of IgG

isotype (Figure 7A and B). In addition, MCT-injected rats receiving anti-CD74 neutralizing antibodies at the dose of 30 µg/kg presented higher values of cardiac output than MCT-injected rats receiving vehicle (Figure 7A). Consistent with our findings obtained with the MIF antagonist ISO-1, levels of endothelial ICAM-1, VCAM-1, E-selectin, levels of circulating IL-6 and MCP-1, and numbers of CD45-, CD3- and CD68-positive cells at day 21 were markedly attenuated in rats treated with anti-CD74 neutralizing antibodies when compared to IgG isotype-treated rats (Figure 7C, 7D, and Supplemental Fig S9 panel B).

**Treatment with ISO-1, in contrast to treatment with anti-CD74 neutralizing antibodies, leads to cardiac fibrosis**

Picrosirius staining of tissue sections of right ventricle myocardium showed increased collagen fibers in endomysium in MCT-injected rats when compared with control rats (Figure 8A and C). We found that this increased right ventricle fibrosis was even more pronounced in MCT-injected rats receiving ISO-1 at the dose of 30 mg/kg when compared with vehicle-treated MCT-injected rats. Interestingly, a substantial reduction in the level of collagen area fraction was observed in the MCT-injected rats treated with anti-CD74 neutralizing antibodies when compared with vehicle-treated MCT-injected rats (Figure 8B and C). Notably, there is no significant difference in collagen area fraction in left ventricle myocardium rats treated or not with ISO-1 or anti-CD74 neutralizing antibodies (Supplemental Fig S10).

## **DISCUSSION**

Both inflammation and pulmonary endothelial dysfunction are intertwined with the initiation and progression of PAH (3, 17, 19). In a series of *in situ*, *in vitro* and *in vivo* experiments, we are reporting novel findings, demonstrating that dysfunctional P-ECs from iPAH patients exhibit a steady state pro-inflammatory phenotype *in situ* and *in vitro*, characterized not only by an increased expression/secretion of key cytokines and chemokines for PAH but also by a marked expression of key cell adhesion molecules. We also found that MIF protein levels are increased in serum of PAH patients as compared to controls and that T-cell lymphocytes

represent a cause of this overabundance. Based on these observations, we hypothesized that the MIF receptor CD74 on the cell surface of P-ECs could contribute to the endothelial pro-inflammatory phenotype in PAH. We found that CD74 is highly expressed in the endothelium of muscularized distal pulmonary arteries as well as in cultured P-ECs from PAH patients and contributes to an exaggerated recruitment of PBMCs to pulmonary PAH ECs. Finally, we found that daily curative treatment of rats with the MIF antagonist ISO-1 or with anti-CD74 neutralizing antibodies started 2 weeks after a subcutaneous MCT injection substantially attenuates the abnormal pulmonary endothelial pro-inflammatory phenotype and partially regresses established PH, assessed by mPAP, right ventricular hypertrophy, and pulmonary arterial muscularization. Thus, we report, for the first time, evidence that the endothelial CD74 signaling system contributes to the steady state pro-inflammatory EC phenotype in PAH, characterized by an abnormal inflammatory mediator release and over-expressions of key adhesion molecules.

The study presented here is the first to provide direct experimental proof that the P-ECs from iPAH patients exhibit a steady state pro-inflammatory phenotype *in situ* and *in vitro*. Among the adhesion molecule positive cells, our data clearly show that the dysfunctional P-ECs from iPAH patients abnormally express high levels of the integrin ligands ICAM-1, VCAM-1, E-selectin, and P-selectin. Together with other altered immune processes, leukocyte recruitment and arrest are central steps in inflammatory reactions and associated diseases, including PAH (29). Histopathologically, pulmonary vascular lesions occurring in patients with PAH as well as in experimental PH are characterized by varying degrees of perivascular inflammatory infiltrates, comprising of T- and B-lymphocytes, macrophages, dendritic and mast cells. Recently, correlations of the average perivascular inflammation score with intima plus media and adventitia thickness respectively, and with mPAP have been found, strongly supporting an important role of perivascular inflammation in the processes of vascular remodeling (29). Beyond altered perivascular accumulation, abnormally elevated circulating levels of certain cytokines and chemokines, i.e. IL-1 $\beta$ , IL-6,

IL-8, CCL2/MCP-1, CX3CL1/fractalkine, CCL5/RANTES and TNF- $\alpha$ , have been reported to correlate with a worse clinical outcome in PAH patients (31, 32). Although we obtained evidences that the dysfunctional pulmonary endothelium partly contributes to the immune/inflammatory component of PAH, other altered processes are known to be critical (3, 33). Here, we showed that primary early (< 3) passage cultures of human ECs established from lung tissue obtained from iPAH patients also expressed high levels of different key cytokines and chemokines, namely IL-1 $\alpha$ , IL-6, IL-8, IL-12, and MCP-1. Although transforming growth factor-beta (TGF- $\beta$ )/ bone morphogenic protein (BMP) signaling is involved in the pathogenesis of PAH and is able to modulate key inflammatory genes (34-37), we did not find any differences between PAH patients carrying a BMP receptor 2 mutation and noncarriers. In addition, we obtained evidences that primary early passage cultures of P-ECs derived from iPAH patients can attract and bind more leukocytes than control cells.

It is known that signaling of MIF through CD74 contributes to inflammation (4-6). Here, we obtained direct evidences that CD74 and its signaling through MIF are key players at the crossroad of inflammation and endothelial dysfunction in the pathogenesis of PAH. Pretreatment with exogenous MIF induces a substantial increases in secretions of endothelial-derived IL-6 and MCP-1 as well as the expressions of adhesion molecules, leading to exaggerated PBMC adhesion on confluent EC monolayers of both iPAH and control P-ECs. The precise mechanism(s) by which the activation of the endothelial CD74 signaling further increases this phenomenon in cultured iPAH cells remain(s) to be determined. We also showed that decreasing CD74 signaling by RNA interference diminished the amount of bound PBMCs on confluent EC monolayers, whereas overexpressing CD74 signaling by a plasmid-based expression vector substantially enhanced this amount of bound PBMCs. Importantly, we also obtained direct *in vitro* evidence demonstrating that ISO-1 and neutralizing antibodies against CD74 are able to decrease the pro-inflammatory signature of P-ECs derived from patients with iPAH. Finally,

we found substantial reduction in levels of ICAM-1, VCAM-1, E-selectin, IL-6 and MCP-1 in lungs of MCT-injected rats treated with ISO-1 and anti-CD74 when compared to MCT-injected rats treated with vehicle. Consistent with these findings, pulmonary infiltration of MCT-injected rats chronically treated with the MIF antagonist ISO-1 or with anti-CD74 neutralizing antibodies is substantially reduced. Consistent with our findings, Zhang and colleagues have also reported that MIF plays a critical role in hypoxia-induced PH and that its inhibition may be beneficial in preventing the development and progression of the hypoxic PH (38, 39). In addition, Bernhagen and colleagues (9) have demonstrated that the inhibition of CD74 with neutralizing antibodies reduced the MIF-dependent monocyte arrest on *ex vivo* carotid arteries from apolipoprotein E-deficient (ApoE<sup>-/-</sup>) mice. Takahashi and colleagues (12) obtained clear evidence that MIF, in the alveolar space, results in neutrophil accumulation *via* activation of CD74. Furthermore, Fan and colleagues (7) have clearly demonstrated that exogenous MIF-induced leukocyte adhesion and transmigration were severely impaired in transgenic mice deficient in CD74. In both the CD74 and MIF deficient mice, it was shown that the MCP-1 induced monocyte arrest and endothelial transmigration were impaired (7). MIF is also known to bind with low nanomolar affinity to chemokine receptors CXCRs (i.e. CXCR2 and CXCR4) that our group has shown to be overexpressed in pulmonary vascular SMCs of chronic hypoxia-exposed mice after development of PH. We reported that AMD3100, a CXCR4 antagonist, alone or combined with CCX771, a CXCR7 antagonist, prevented vascular remodeling, PH and perivascular accumulation of c-kit<sup>+</sup>/sca-1<sup>+</sup> progenitor cells, with a synergistic effect of these agents (40). In contrast, herein, no difference in the relative mRNA levels of CXCR2 and CXCR4 were found in P-ECs from controls and iPAH patients. Consistently, no difference was observed in the relative mRNA levels of ICAM-1, VCAM-1 and E-selectin in iPAH P-ECs treated or not with CXCR2 and CXCR4 antagonists (SB225002 and AMD3100, respectively). These findings support the notion that in P-ECs MIF/CD74, but MIF/CXCR2 or MIF/CXCR4, is an important axis for the aberrant pro-inflammatory EC phenotype in iPAH. Using the MIF inhibitor ISO-1, we could not exclude the possibility that the observed beneficial effects were also due to the inhibition

of CXCR signaling in SMCs. These data are the rationale for using a neutralizing antibody against CD74 in our model to specifically demonstrate the contribution of the MIF/CD74 pathway in the progression of PH and its therapeutical potential.

CD74 is present in limited amounts in the pulmonary endothelium of control lung tissues but overexpressed in the endothelium of remodeled vessels in iPAH patient lungs, supporting the hypothesis that it is an attractive target for therapy. In normal tissues, expression of CD74 is known to be limited to B cells, monocytes, macrophages, dendritic cells and epithelial cells of endodermal and mesodermal origin (24). Consistent with this knowledge, several CD74 positive cells are found in the perivascular area in the pulmonary endothelium of normal and iPAH lung tissues. However, our results also showed strong CD74 staining within the endothelium of distal-pulmonary arteries from iPAH patients, contrasting with a negative or a weak staining for CD74 in control lung tissues. Here, we found that ISO-1 and neutralizing antibodies against CD74 are able to decrease the pro-inflammatory signature of P-ECs derived from patients with iPAH. In addition, daily treatment of rats with the MIF antagonist ISO-1 or with anti-CD74 neutralizing antibodies started 2 weeks after a subcutaneous MCT injection partially regress established PH, assessed by mPAP, right ventricular hypertrophy, percentage of medial wall thickness and pulmonary arterial muscularization. Since MIF/ CD74 signaling is not restricted to the endothelial layer, we cannot exclude that beneficial effects observed *in vivo* with ISO-1 and neutralizing antibodies against CD74 are due to actions on other cell-types and not only on dysfunctional P-ECs. Although we noted a mild beneficial effect of anti-CD74 neutralizing antibody treatment on pulmonary hemodynamics, levels of endothelial ICAM-1, VCAM-1, E-selectin, levels of circulating IL-6 and MCP-1, and numbers of CD45-, CD3- and CD68-positive cells at day 21 were markedly attenuated. It is believed that initial inflammatory mononuclear infiltration is mainly driven by the acute vascular injury induced by monocrotaline-pyrrole (21). In contrast, in the following phases of the animal model, a chronic inflammation takes place and contributes to PA-SMC proliferation and subsequent vascular remodeling, which result in

pulmonary hypertension, and finally, in right ventricular failure (3, 21, 33). Therefore, our results underlie the importance of MIF/CD74 signaling pathway in the progression of the disease, offering a valuable therapeutical target.

The potential impact of therapeutic molecules on heart function and adaptive responses is an important concern in patients with PH. In order to verify the translational potential of anti-CD74 strategies (ISO-1 and anti-CD74) and since MIF modulates the activation of the cardio-protective AMPK pathway during ischemia, we wanted to assess their cardiac effects in our *in vivo* studies. We found that blocking MIF in MCT-injected rats with ISO-1, but not with anti-CD74 neutralizing antibodies, can aggravate the reduction in cardiac output and lead to cardiac fibrosis. Consistent with our findings, Kiyokazu Koga and collaborators (41) have demonstrated that loss of the intrinsic oxidoreductase activity of MIF in the heart results in augmented cardiac hypertrophy in response to hemodynamic stress, supporting the notion that this activity is important in maintaining redox homeostasis (42). Therefore, further studies are needed to better understand the effect of MIF inhibition in chronic heart disease. Moreover, substantial work remains to be done to discover and/or develop new, better-tolerated and more powerful therapeutic small molecules to inhibit MIF/CD74 signaling system.

In summary, our study provides the first *in situ* and *in vitro* demonstration that P-ECs from iPAH patients exhibit a steady state pro-inflammatory phenotype. Furthermore, our findings underscore for the first time the critical role of endothelial CD74 signaling in this process. Chronic treatment with the MIF antagonist ISO-1 or with anti-CD74 neutralizing antibodies in the MCT-induced PH model revealed reduced disease progression, decreased pulmonary infiltration and vascular remodeling. We therefore report strong evidence that MIF and its signaling through endothelial CD74 could be key players at the crossroad of inflammation, cancer-like phenotype and endothelial dysfunction in PAH pathogenesis.

**Acknowledgments:** We would like to thank Pr. Richard Bucala for kindly providing the pcDNA3.1-CD74 plasmid. We also thank Dr. Elodie Gouadon and Dr. Veronique Capuano for their very helpful technical assistance. Finally, we would like to thank Dr. Gaël Jalce from MIFCARE (School of medicine, Paris Descartes University, Paris, France) for the synthesis of ISO-1.

**Conflict of interest**

None.

**Disclosures**

None.

**Abbreviations:**

*α-smooth muscle actin: **α-SMA**; arbitrary unit: **AU**; clusters of differentiation: **CD**; control: **CTR**; D-dopachrome tautomerase: **DDT**; endothelial cell: **EC**; interleukin: **IL**; intercellular adhesion molecule-1: **ICAM-1**; major histocompatibility complex: **MHC**; mean pulmonary arterial pressure: **mPAP**; monocrotaline: **MCT**; monocyte chemotactic protein: **MCP-1**; macrophage migration inhibitory factor: **MIF**; peripheral blood mononuclear cells: **PBMCs**; pulmonary arterial hypertension: **PAH**; right ventricular hypertrophy: **RVH**; right ventricular systolic pressure: **RVSP**; vascular cell adhesion molecule-1: **VCAM-1**.*

## References:

1. Humbert M, Sitbon O, Chaouat A, Bertocchi M, Habib G, Gressin V, Yaici A, Weitzenblum E, Cordier JF, Chabot F, Dromer C, Pison C, Reynaud-Gaubert M, Haloun A, Laurent M, Hachulla E, Cottin V, Degano B, Jais X, Montani D, Souza R, Simonneau G. Survival in patients with idiopathic, familial, and anorexigen-associated pulmonary arterial hypertension in the modern management era. *Circulation* 2010; 122: 156-163.
2. Voelkel NF, Gomez-Arroyo J, Abbate A, Bogaard HJ, Nicolls MR. Pathobiology of pulmonary arterial hypertension and right ventricular failure. *The European respiratory journal* 2012; 40: 1555-1565.
3. Huertas A, Perros F, Tu L, Cohen-Kaminsky S, Montani D, Dorfmüller P, Guignabert C, Humbert M. Immune dysregulation and endothelial dysfunction in pulmonary arterial hypertension: a complex interplay. *Circulation* 2014; 129: 1332-1340.
4. Leng L, Metz CN, Fang Y, Xu J, Donnelly S, Baugh J, Delohery T, Chen Y, Mitchell RA, Bucala R. MIF signal transduction initiated by binding to CD74. *The Journal of experimental medicine* 2003; 197: 1467-1476.
5. Tillmann S, Bernhagen J, Noels H. Arrest Functions of the MIF Ligand/Receptor Axes in Atherogenesis. *Frontiers in immunology* 2013; 4: 115.
6. Gregory JL, Morand EF, McKeown SJ, Ralph JA, Hall P, Yang YH, McColl SR, Hickey MJ. Macrophage migration inhibitory factor induces macrophage recruitment via CC chemokine ligand 2. *J Immunol* 2006; 177: 8072-8079.
7. Fan H, Hall P, Santos LL, Gregory JL, Fingerle-Rowson G, Bucala R, Morand EF, Hickey MJ. Macrophage migration inhibitory factor and CD74 regulate macrophage chemotactic responses via MAPK and Rho GTPase. *J Immunol* 2011; 186: 4915-4924.
8. Miller EJ, Li J, Leng L, McDonald C, Atsumi T, Bucala R, Young LH. Macrophage migration inhibitory factor stimulates AMP-activated protein kinase in the ischaemic heart. *Nature* 2008; 451: 578-582.

9. Bernhagen J, Krohn R, Lue H, Gregory JL, Zerneck A, Koenen RR, Dewor M, Georgiev I, Schober A, Leng L, Kooistra T, Fingerle-Rowson G, Ghezzi P, Kleemann R, McColl SR, Bucala R, Hickey MJ, Weber C. MIF is a noncognate ligand of CXC chemokine receptors in inflammatory and atherogenic cell recruitment. *Nature medicine* 2007; 13: 587-596.
10. Damico R, Simms T, Kim BS, Tekeste Z, Amankwan H, Damarla M, Hassoun PM. p53 mediates cigarette smoke-induced apoptosis of pulmonary endothelial cells: inhibitory effects of macrophage migration inhibitor factor. *American journal of respiratory cell and molecular biology* 2011; 44: 323-332.
11. Lue H, Thiele M, Franz J, Dahl E, Speckgens S, Leng L, Fingerle-Rowson G, Bucala R, Luscher B, Bernhagen J. Macrophage migration inhibitory factor (MIF) promotes cell survival by activation of the Akt pathway and role for CSN5/JAB1 in the control of autocrine MIF activity. *Oncogene* 2007; 26: 5046-5059.
12. Takahashi K, Koga K, Linge HM, Zhang Y, Lin X, Metz CN, Al-Abed Y, Ojamaa K, Miller EJ. Macrophage CD74 contributes to MIF-induced pulmonary inflammation. *Respiratory research* 2009; 10: 33.
13. Gore Y, Starlets D, Maharshak N, Becker-Herman S, Kaneyuki U, Leng L, Bucala R, Shachar I. Macrophage migration inhibitory factor induces B cell survival by activation of a CD74-CD44 receptor complex. *The Journal of biological chemistry* 2008; 283: 2784-2792.
14. de Man FS, Tu L, Handoko ML, Rain S, Ruiters G, Francois C, Scholij I, Dorfmueller P, Simonneau G, Fadel E, Perros F, Boonstra A, Postmus PE, van der Velden J, Vonk-Noordegraaf A, Humbert M, Eddahibi S, Guignabert C. Dysregulated renin-angiotensin-aldosterone system contributes to pulmonary arterial hypertension. *American journal of respiratory and critical care medicine* 2012; 186: 780-789.
15. Guignabert C, Tu L, Izikki M, Dewachter L, Zadigue P, Humbert M, Adnot S, Fadel E, Eddahibi S. Dichloroacetate treatment partially regresses established pulmonary hypertension in mice with SM22alpha-targeted overexpression of the serotonin

- transporter. *FASEB journal : official publication of the Federation of American Societies for Experimental Biology* 2009; 23: 4135-4147.
16. Huertas A, Tu L, Gambaryan N, Girerd B, Perros F, Montani D, Fabre D, Fadel E, Eddahibi S, Cohen-Kaminsky S, Guignabert C, Humbert M. Leptin and regulatory T-lymphocytes in idiopathic pulmonary arterial hypertension. *The European respiratory journal* 2012; 40: 895-904.
  17. Ricard N, Tu L, Le Hires M, Huertas A, Phan C, Thuillet R, Sattler C, Fadel E, Seferian A, Montani D, Dorfmuller P, Humbert M, Guignabert C. Increased pericyte coverage mediated by endothelial-derived fibroblast growth factor-2 and interleukin-6 is a source of smooth muscle-like cells in pulmonary hypertension. *Circulation* 2014; 129: 1586-1597.
  18. Tu L, De Man FS, Girerd B, Huertas A, Chaumais MC, Lecerf F, Francois C, Perros F, Dorfmuller P, Fadel E, Montani D, Eddahibi S, Humbert M, Guignabert C. A critical role for p130Cas in the progression of pulmonary hypertension in humans and rodents. *American journal of respiratory and critical care medicine* 2012; 186: 666-676.
  19. Tu L, Dewachter L, Gore B, Fadel E, Dartevielle P, Simonneau G, Humbert M, Eddahibi S, Guignabert C. Autocrine fibroblast growth factor-2 signaling contributes to altered endothelial phenotype in pulmonary hypertension. *American journal of respiratory cell and molecular biology* 2011; 45: 311-322.
  20. Binsky I, Haran M, Starlets D, Gore Y, Lantner F, Harpaz N, Leng L, Goldenberg DM, Shvidel L, Berrebi A, Bucala R, Shachar I. IL-8 secreted in a macrophage migration-inhibitory factor- and CD74-dependent manner regulates B cell chronic lymphocytic leukemia survival. *Proceedings of the National Academy of Sciences of the United States of America* 2007; 104: 13408-13413.
  21. Guignabert C, Raffestin B, Benferhat R, Raoul W, Zadigue P, Rideau D, Hamon M, Adnot S, Eddahibi S. Serotonin transporter inhibition prevents and reverses

- monocrotaline-induced pulmonary hypertension in rats. *Circulation* 2005; 111: 2812-2819.
22. El-Bizri N, Guignabert C, Wang L, Cheng A, Stankunas K, Chang CP, Mishina Y, Rabinovitch M. SM22alpha-targeted deletion of bone morphogenetic protein receptor 1A in mice impairs cardiac and vascular development, and influences organogenesis. *Development* 2008; 135: 2981-2991.
23. Guignabert C, Alvira CM, Alastalo TP, Sawada H, Hansmann G, Zhao M, Wang L, El-Bizri N, Rabinovitch M. Tie2-mediated loss of peroxisome proliferator-activated receptor-gamma in mice causes PDGF receptor-beta-dependent pulmonary arterial muscularization. *American journal of physiology Lung cellular and molecular physiology* 2009; 297: L1082-1090.
24. Badve S, Deshpande C, Hua Z, Logdberg L. Expression of invariant chain (CD 74) and major histocompatibility complex (MHC) class II antigens in the human fetus. *The journal of histochemistry and cytochemistry : official journal of the Histochemistry Society* 2002; 50: 473-482.
25. Pyrz M, Wang B, Wabl M, Pedersen FS. A retroviral mutagenesis screen identifies Cd74 as a common insertion site in murine B-lymphomas and reveals the existence of a novel IFNgamma-inducible Cd74 isoform. *Molecular cancer* 2010; 9: 86.
26. Richard V, Kindt N, Decaestecker C, Gabius HJ, Laurent G, Noel JC, Saussez S. Involvement of macrophage migration inhibitory factor and its receptor (CD74) in human breast cancer. *Oncology reports* 2014; 32: 523-529.
27. Eriksson EE. Mechanisms of leukocyte recruitment to atherosclerotic lesions: future prospects. *Current opinion in lipidology* 2004; 15: 553-558.
28. Davis BB, Shen YH, Tancredi DJ, Flores V, Davis RP, Pinkerton KE. Leukocytes are recruited through the bronchial circulation to the lung in a spontaneously hypertensive rat model of COPD. *PLoS one* 2012; 7: e33304.
29. Stacher E, Graham BB, Hunt JM, Gandjeva A, Groshong SD, McLaughlin VV, Jessup M, Grizzle WE, Aldred MA, Cool CD, Tudor RM. Modern age pathology of pulmonary

- arterial hypertension. *American journal of respiratory and critical care medicine* 2012; 186: 261-272.
30. Vera PL, Wang X, Bucala RJ, Meyer-Siegler KL. Intraluminal blockade of cell-surface CD74 and glucose regulated protein 78 prevents substance P-induced bladder inflammatory changes in the rat. *PloS one* 2009; 4: e5835.
  31. Cracowski JL, Chabot F, Labarere J, Faure P, Degano B, Schwebel C, Chaouat A, Reynaud-Gaubert M, Cracowski C, Sitbon O, Yaici A, Simonneau G, Humbert M. Proinflammatory cytokine levels are linked with death in pulmonary arterial hypertension. *The European respiratory journal* 2013.
  32. Soon E, Holmes AM, Treacy CM, Doughty NJ, Southgate L, Machado RD, Trembath RC, Jennings S, Barker L, Nicklin P, Walker C, Budd DC, Pepke-Zaba J, Morrell NW. Elevated levels of inflammatory cytokines predict survival in idiopathic and familial pulmonary arterial hypertension. *Circulation* 2010; 122: 920-927.
  33. Rabinovitch M, Guignabert C, Humbert M, Nicolls MR. Inflammation and immunity in the pathogenesis of pulmonary arterial hypertension. *Circulation research* 2014; 115: 165-175.
  34. Sorescu GP, Sykes M, Weiss D, Platt MO, Saha A, Hwang J, Boyd N, Boo YC, Vega JD, Taylor WR, Jo H. Bone morphogenic protein 4 produced in endothelial cells by oscillatory shear stress stimulates an inflammatory response. *The Journal of biological chemistry* 2003; 278: 31128-31135.
  35. Csiszar A, Ahmad M, Smith KE, Labinsky N, Gao Q, Kaley G, Edwards JG, Wolin MS, Ungvari Z. Bone morphogenetic protein-2 induces proinflammatory endothelial phenotype. *The American journal of pathology* 2006; 168: 629-638.
  36. Davies RJ, Holmes AM, Deighton J, Long L, Yang X, Barker L, Walker C, Budd DC, Upton PD, Morrell NW. BMP type II receptor deficiency confers resistance to growth inhibition by TGF-beta in pulmonary artery smooth muscle cells: role of proinflammatory cytokines. *American journal of physiology Lung cellular and molecular physiology* 2012; 302: L604-615.

37. Helbing T, Rothweiler R, Ketterer E, Goetz L, Heinke J, Grundmann S, Duerschmied D, Patterson C, Bode C, Moser M. BMP activity controlled by BMPER regulates the proinflammatory phenotype of endothelium. *Blood* 2011; 118: 5040-5049.
38. Zhang B, Shen M, Xu M, Liu LL, Luo Y, Xu DQ, Wang YX, Liu ML, Liu Y, Dong HY, Zhao PT, Li ZC. Role of macrophage migration inhibitory factor in the proliferation of smooth muscle cell in pulmonary hypertension. *Mediators of inflammation* 2012; 2012: 840737.
39. Zhang Y, Talwar A, Tsang D, Bruchfeld A, Sadoughi A, Hu M, Omonuwa K, Cheng KF, Al-Abed Y, Miller EJ. Macrophage migration inhibitory factor mediates hypoxia-induced pulmonary hypertension. *Mol Med* 2012; 18: 215-223.
40. Gambaryan N, Perros F, Montani D, Cohen-Kaminsky S, Mazmanian M, Renaud JF, Simonneau G, Lombet A, Humbert M. Targeting of c-kit<sup>+</sup> haematopoietic progenitor cells prevents hypoxic pulmonary hypertension. *The European respiratory journal* 2011; 37: 1392-1399.
41. Koga K, Kenessey A, Ojamaa K. Macrophage migration inhibitory factor antagonizes pressure overload-induced cardiac hypertrophy. *American journal of physiology Heart and circulatory physiology* 2013; 304: H282-293.
42. Schober A, Bernhagen J, Thiele M, Zeiffer U, Knarren S, Roller M, Bucala R, Weber C. Stabilization of atherosclerotic plaques by blockade of macrophage migration inhibitory factor after vascular injury in apolipoprotein E-deficient mice. *Circulation* 2004; 109: 380-385.

## FIGURE LEGENDS

**Figure 1. Increased expressions of adhesion molecules in endothelium of pulmonary arteries in human idiopathic pulmonary arterial hypertension (iPAH).** Representative images of intercellular adhesion molecule (ICAM)-1 (red) **(A)**, vascular cell adhesion molecule (VCAM)-1 (red) **(B)**, and E-selectin (red) **(C)** in pulmonary endothelial cells (positive for von Willebrand factor (vWF); green) in lungs from control (CTR) subjects and patients with iPAH. **D:** Quantification of the intensity of fluorescence for endothelial ICAM-1, VCAM-1 and E-selectin in vWF<sup>+</sup> cells of 5-10 remodeled vessels per subject (n=5 control subjects and n=5 patients with iPAH). The bar graph represents means  $\pm$  SEM. \* p-value < 0.05; \*\* p-value < 0.01 compared with CTR. Scale bar = 50  $\mu$ m in all sections.

**Figure 2. Pulmonary endothelial cells (P-ECs) from idiopathic pulmonary arterial hypertension (iPAH) patients exhibit a steady state pro-inflammatory phenotype. A:** Gene expression analysis of primary early (< 3) passage cultures of human P-ECs established from lung tissue obtained from control (CTR) and iPAH patients. **B:** Effects of conditioned media of quiescent cultured human P-ECs from CTR and iPAH patients on the migratory capacity of peripheral blood mononuclear cells (PBMCs). The left part of the panel contains two representative FACS dot plots obtained from migrating PBMCs in the lower compartment of the modified Boyden chamber stained with Hoechst 33342. Quantification is shown in the right panel. **C:** Adhesion of PBMCs (stained using green-fluorescent Oregon Green® 488 wheat germ agglutinin) to confluent monolayers of P-ECs from CTR and iPAH patients (stained using CellTracker™ Red CMTPIX). The bar graph represents means  $\pm$  SEM (n= 4-8, where n represents the number of patients). \* p-value < 0.05; \*\* p-value < 0.01; \*\*\* p-value < 0.001 compared with CTR P-ECs. Scale bar = 20  $\mu$ m in all sections. NS: non significant; FSC: forward scatter.

**Figure 3. Dysregulation of the MIF/ CD74 signaling pathway in pulmonary arterial hypertension (PAH).** **A:** Levels of circulating MIF (left panel) and D-dopachrome tautomerase (DDT) (right panel) proteins in the serum of patients with PAH compared with

those from controls (CTR). **B:** Quantification of mean fluorescence intensity of MIF intracellular content in CD3 (T lymphocytes), CD19 (B lymphocytes), and CD14 (monocytes) positive cells by FACS using dual labeling of human PBMCs. **C:** Representative photomicrographs of CD74 immunostaining in distal pulmonary arteries in lung sections from CTR and iPAH patients. **D:** Representative Western blots and quantification of the CD74/ $\beta$ -actin ratio in pulmonary endothelial cells (P-ECs) from CTR and iPAH patients. Values are means  $\pm$  SEM (n= 5-40, where n represents the number of patients). \*\* p-value < 0.01; \*\*\* p-value < 0.001 compared with CTR P-ECs. Scale bar = 20  $\mu$ m in all sections. NS= non significant.

**Figure 4. MIF/ CD74 is involved in the endothelial pro-inflammatory phenotype and leukocyte recruitment in pulmonary arterial hypertension (PAH).** **A:** Representative images of E-selectin, vascular cell adhesion molecule (VCAM)-1 and intercellular adhesion molecule (ICAM)-1 labeling in control (CTR) pulmonary endothelial cells (P-ECs) treated or not for 24 h with 100ng/mL of MIF [included measurements of mean fluorescence intensity (means  $\pm$  SEM)]. **B:** Secretions of IL-6 and MCP-1 in conditioned media of CTR P-ECs treated or not for 24 h with 100ng/mL of MIF. **C:** Adhesion of PBMCs to confluent monolayers of CTR and idiopathic (i)PAH P-ECs with or without a pretreatment for 24 h with 100ng/mL of MIF (left panel: representative images; right panel: quantification). **D:** Adhesion of PBMCs to confluent monolayers of P-ECs from CTR with or without CD74 inhibition by RNA-interference and with or without CD74 overexpression using the pcDNA3.1/v5-His/CD74 plasmid or the pcDNA3.1/v5-His/LacZ plasmid (left panel: representative images; right panels: quantification). **E:** Gene expression analyses of primary early (< 3) passage cultures of human P-ECs derived from iPAH patients treated or not with ISO-1 (10, 50, and 100  $\mu$ M; n=3 patients), anti-IgG isotype, anti-CD74 neutralizing antibodies (30  $\mu$ g/mL; n=3 patients), or vehicle (n=3 patients). Values are means  $\pm$  SEM (n= 3-7, where n represents the number of patients). \* p-value < 0.05; \*\* p-value < 0.01 compared with untreated CTR P-

ECs, cells transfected with the scrambled sequence, pcDNA3.1/v5-His/LacZ plasmid, iPAH P-ECs + Vehicle, or iPAH P-ECs + IgG isotype. Scale bar = 20  $\mu$ m in all sections.

**Figure 5. Dysregulation of the MIF/ CD74 signaling pathway in two animal models of pulmonary hypertension (PH).** **A:** Levels of circulating MIF proteins in the serum of control animals, chronic hypoxia-exposed animals, and monocrotaline (MCT)-injected rats. **B:** Representative Western blots and quantification of the CD74/ $\beta$ -actin ratio in lungs from MCT-injected rats (from Day-0 to Day-21). **C:** Representative photomicrographs of CD74 immunostaining in distal pulmonary arteries in lung sections from control animals and MCT-injected rats. **D:** Representative FACS dot plots of CD74 expression in von Willebrand factor (vWF) positive cells in collagenase-digested lung tissues from control and MCT-injected rat. The right panel represents the percentage of CD74<sup>+</sup> vWF<sup>+</sup> cells. Values are means  $\pm$  SEM (n= 4-13, where n represents the number of rats). \* p-value < 0.05; \*\*\* p-value < 0.001 compared with vehicle-injected rats. # p-value < 0.05 compared with MCT-injected rats at Day-14. Scale bar = 50  $\mu$ m in all sections.

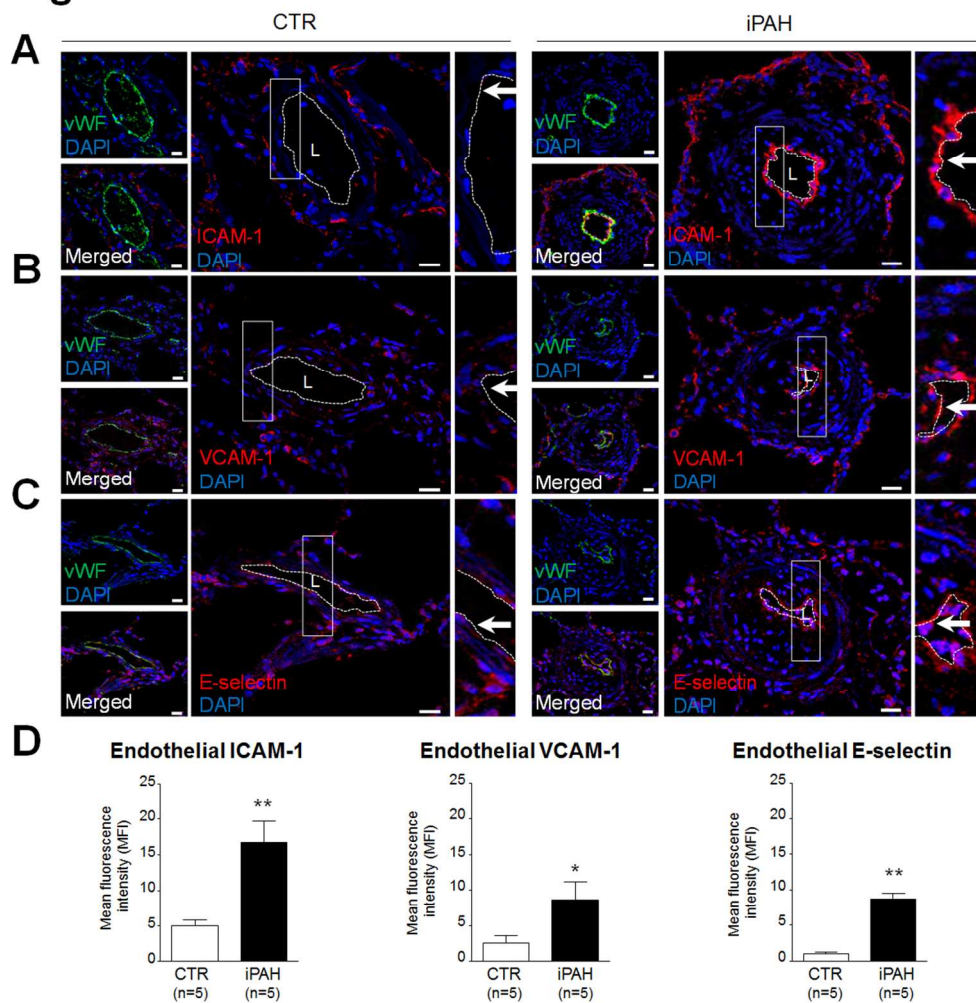
**Figure 6. Evaluation of the efficacy of ISO-1 treatment on the progression of monocrotaline (MCT)-induced pulmonary hypertension (PH) and on the abnormal pulmonary endothelial pro-inflammatory phenotype.** **A:** Top panel: experimental design; Lower panels: mean pulmonary arterial pressure (mPAP), Fulton index, and cardiac output. **B:** Representative images of hematoxylin-eosin (H&E) staining and alpha smooth muscle-actin ( $\alpha$ SMA) (left panel) and quantification of the percentage medial wall thickness and the percentage of muscularized distal pulmonary arteries (right panel). **C:** Representative images and quantifications of immunostainings in rat lungs for intercellular adhesion molecule (ICAM)-1, vascular cell adhesion molecule (VCAM)-1 and E-selectin in vehicle- or MCT-injected rats treated or not with ISO-1 or vehicle. **D:** Levels of circulating IL-6 and MCP-1 proteins in the serum of vehicle- or MCT-injected rats treated or not with ISO-1 or vehicle. Values are means  $\pm$  SEM (n= 3-7, where n represents the number of rats). \* p-value < 0.05; \*\* p-value < 0.01; \*\*\* p-value < 0.001 compared with vehicle-injected rats. # p-value < 0.05;

## p-value < 0.01 compared with MCT-injected rats. Scale bar = 50  $\mu$ m in all sections. NS= non significant.

**Figure 7. Evaluation of the efficacy of anti-CD74 neutralizing antibodies treatment on the progression of monocrotaline (MCT)-induced PH and on the abnormal pulmonary endothelial pro-inflammatory phenotype.** **A:** Top panel: experimental design; Lower panels: mean pulmonary arterial pressure (mPAP), Fulton index, and cardiac output. **B:** Representative images of hematoxylin-eosin (H&E) staining and alpha-smooth muscle actin ( $\alpha$ SMA) and quantification of the percentage medial wall thickness and the percentage of muscularized distal pulmonary arteries. **C:** Representative images and quantifications of immunostainings in rat lungs for intercellular adhesion molecule (ICAM)-1, vascular cell adhesion molecule (VCAM)-1 and E-selectin in vehicle- or MCT-injected rats treated or not with anti-CD74 neutralizing antibodies or IgG isotype. **D:** Levels of circulating IL-6 and MCP-1 proteins in the serum of vehicle- or monocrotaline-injected rats treated or not with anti-CD74 neutralizing antibodies or IgG isotype. Values are means  $\pm$  SEM (n= 3-9, where n represents the number of rats). \* p-value < 0.05; \*\* p-value < 0.01; \*\*\* p-value < 0.001 compared with vehicle-injected rats. # p-value < 0.05; ## p-value < 0.01; compared with MCT-injected rats treated or no with IgG isotype. Scale bar = 50  $\mu$ m in all sections.

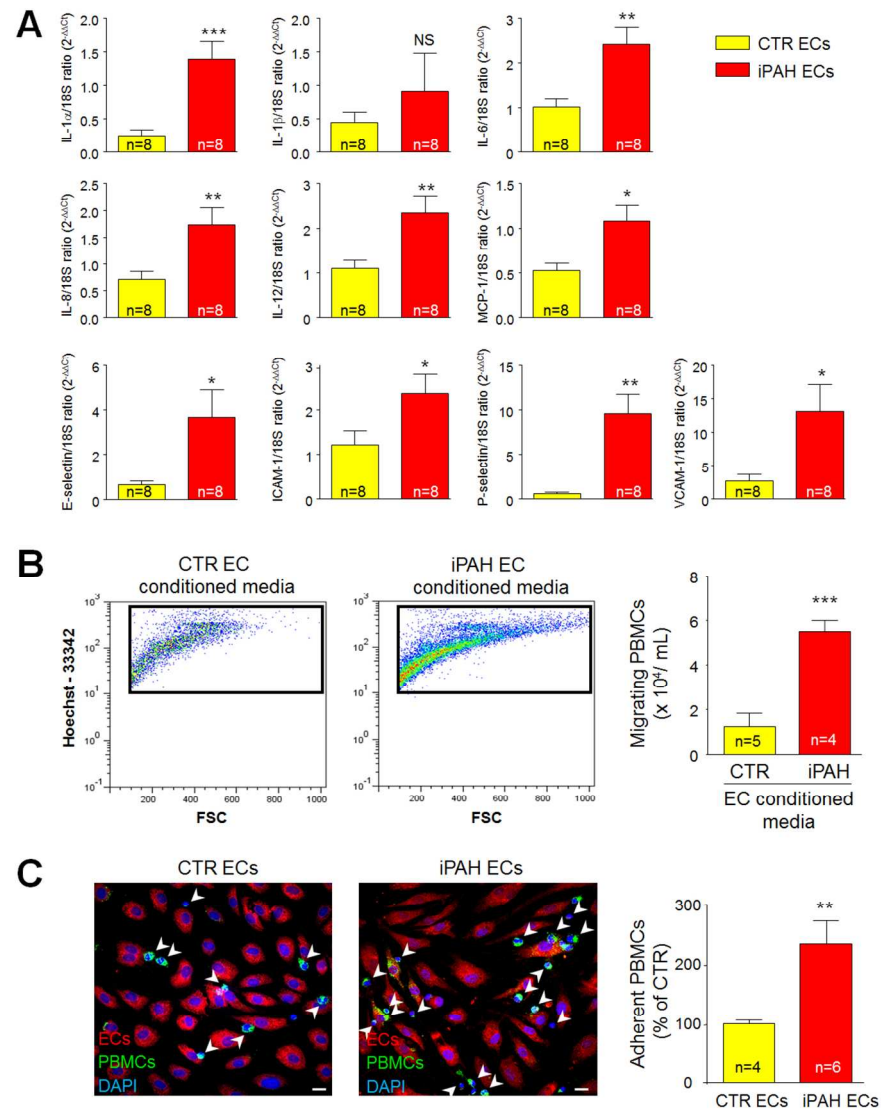
**Figure 8. Evaluation of cardiac fibrosis in right ventricle myocardium of rats treated or not with ISO-1, anti-IgG isotype, or anti-CD74 neutralizing antibodies.** **A:** Representative images of picrosirius staining of tissue section of right ventricle myocardium of control and monocrotaline (MCT)-injected rats treated with ISO-1. **B:** Representative images of picrosirius staining of tissue section of right ventricle myocardium of control and MCT-injected rats treated with anti-IgG isotype, or anti-CD74 neutralizing antibodies. **C:** Quantification of the collagen area fraction in control and MCT-injected rats treated or not with ISO-1, vehicle, anti-CD74 neutralizing antibodies or IgG isotype. Values are means  $\pm$  SEM (n= 7, where n represents the number of rats). \*\* p-value < 0.01, \*\*\* p-value < 0.001 compared with vehicle-injected rats. # p-value < 0.05 compared with MCT-injected rats. Scale bar = 100  $\mu$ m in all sections. NS= non significant.

Fig 1.



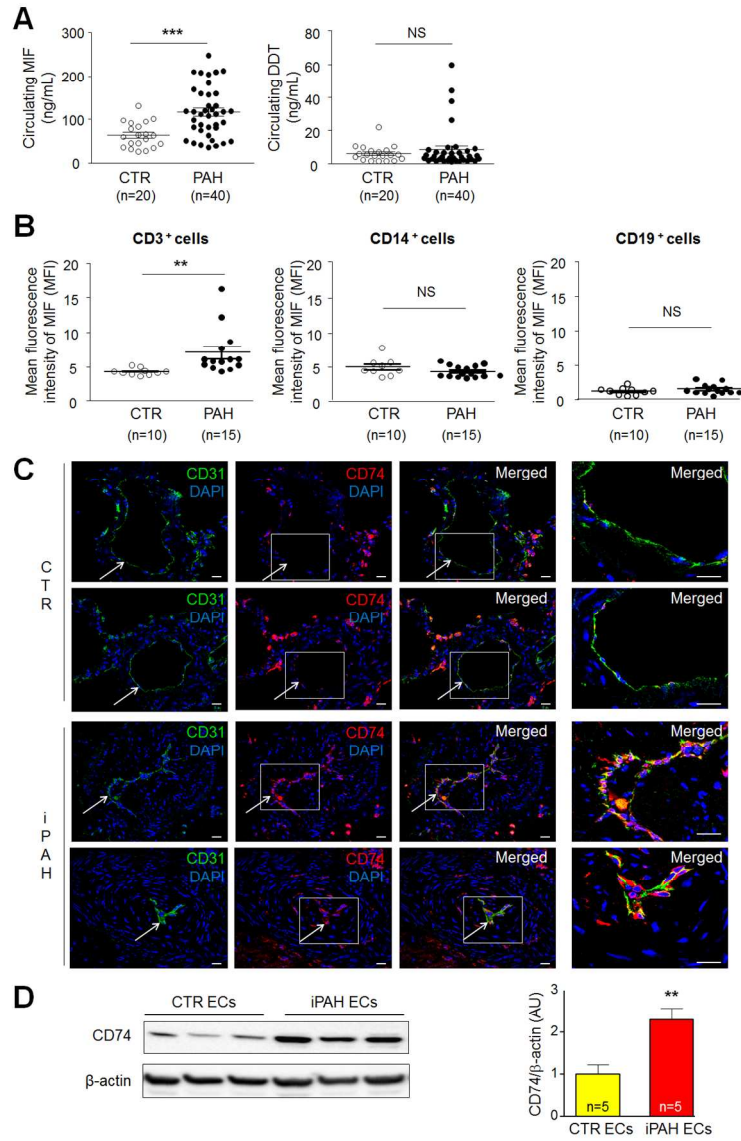
103x110mm (300 x 300 DPI)

Fig 2.



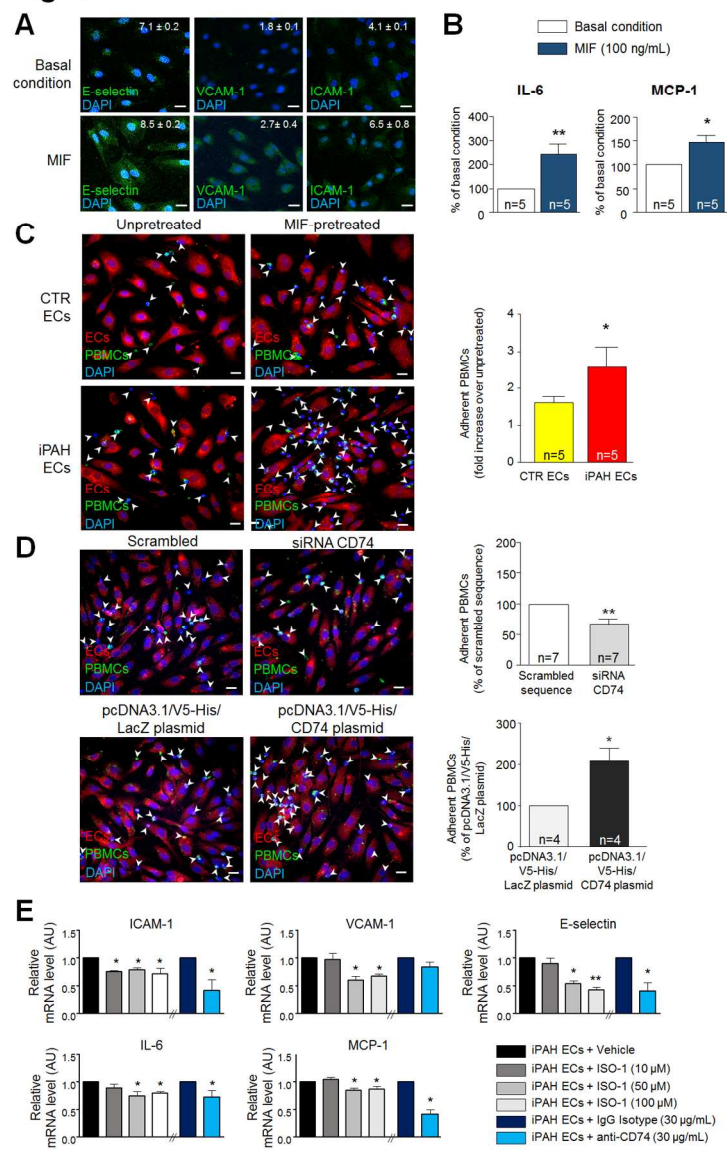
102x136mm (300 x 300 DPI)

Fig 3.



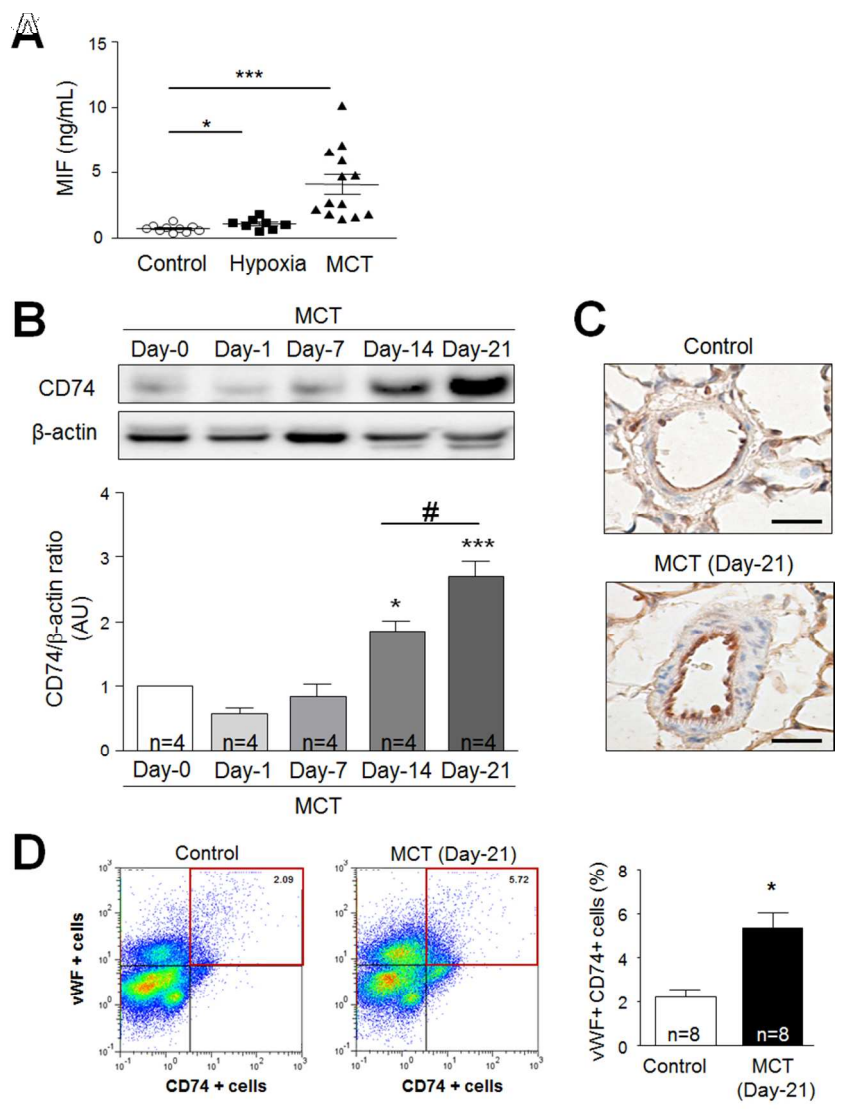
107x171mm (300 x 300 DPI)

Fig 4.



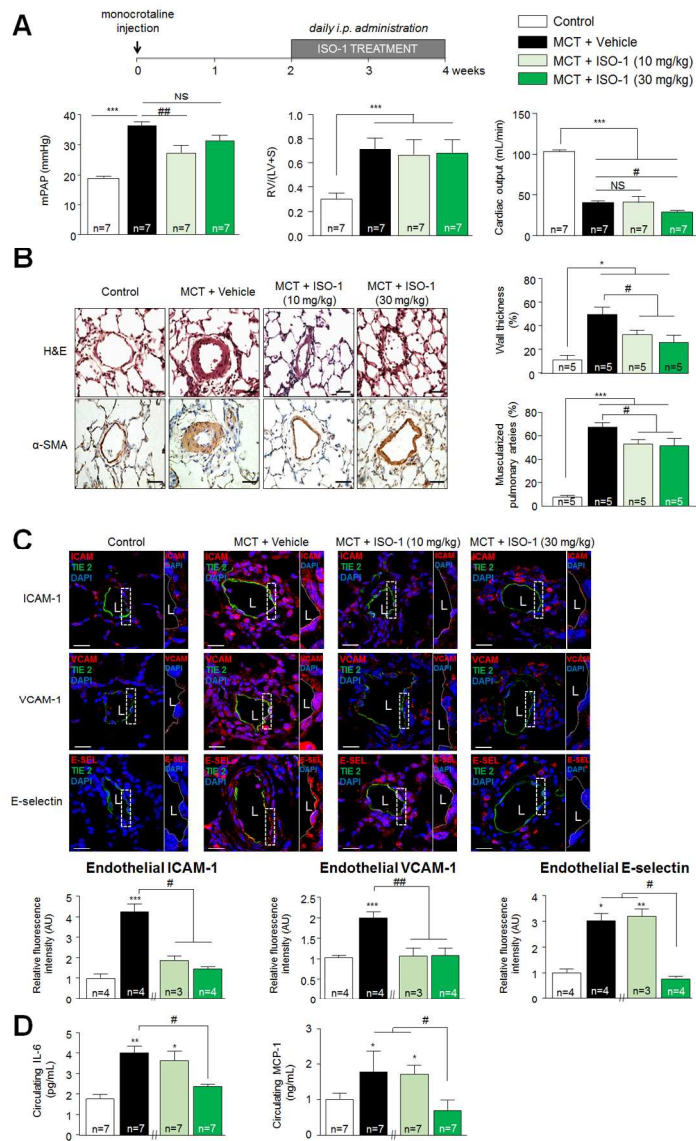
109x179mm (300 x 300 DPI)

Fig 5.



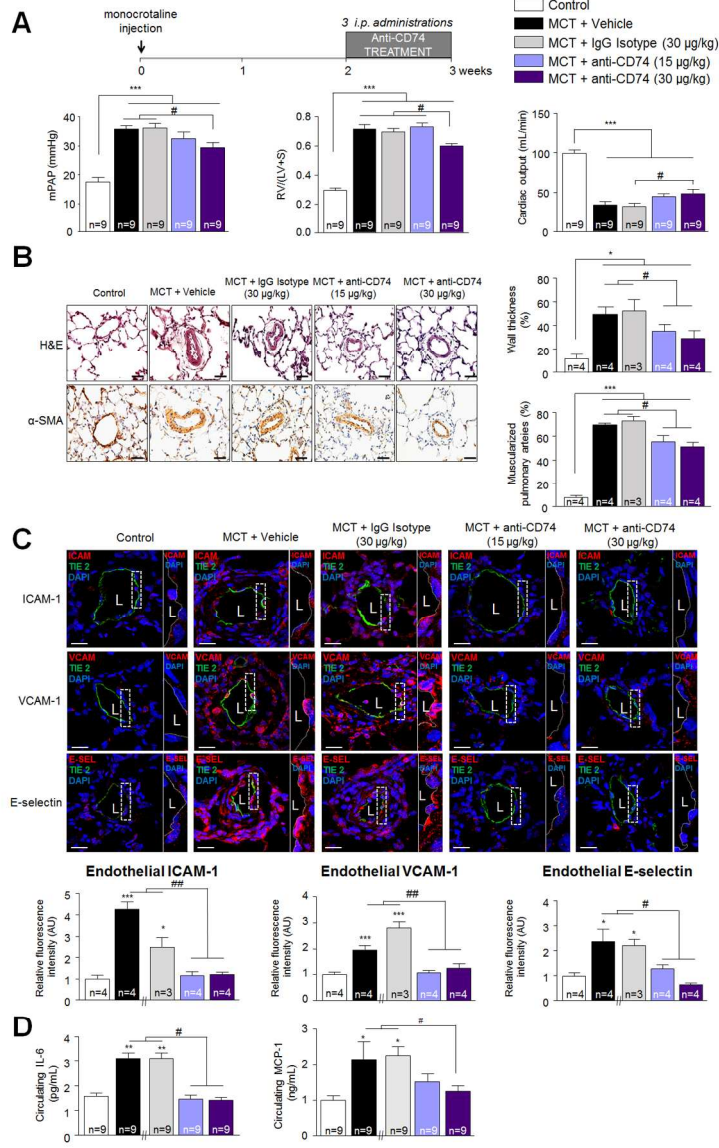
76x107mm (300 x 300 DPI)

Fig 6.



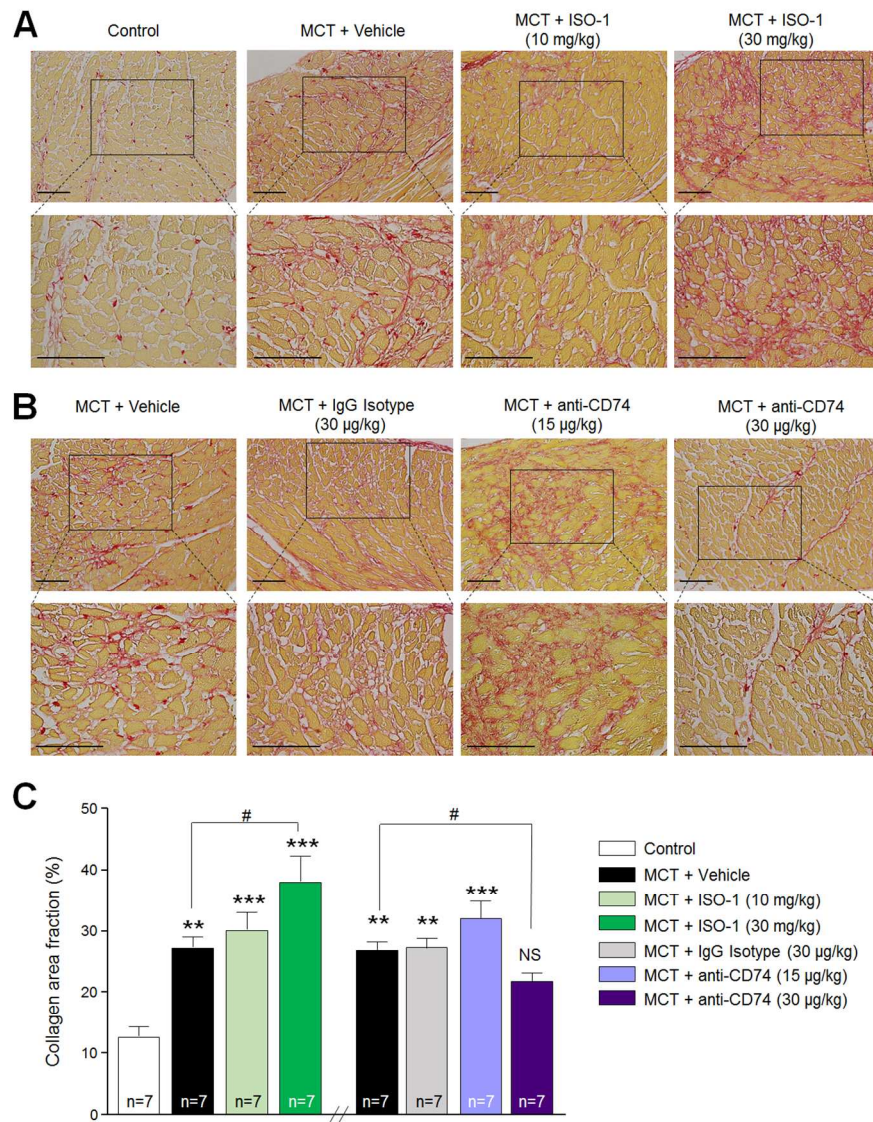
107x182mm (300 x 300 DPI)

**Fig 7.**



111x181mm (300 x 300 DPI)

Fig 8.



107x144mm (300 x 300 DPI)

**Supplemental Table 1** – Characteristics Of Controls And Patients With Idiopathic Pulmonary Arterial Hypertension (iPAH) Before Lung Transplantation:

	<b>iPAH</b> n=8	<b>Controls</b> n=8
<b>Age, yrs</b>	40.9 ± 2.1	58.2 ± 5.3
<b>Sex, M/F (ratio)</b>	2 / 6 (0.33)	3 / 5 (0.60)
<b>NYHA functional class, n</b>		
class II	1	NA
class III	5	NA
class IV	2	NA
<b>mPAP, mmHg</b>	53.6 ± 3.6	NA
<b>CI, l/min/m<sup>2</sup></b>	3 ± 0.2	NA
<b>PVRi, mmHg/l/min/m<sup>2</sup></b>	9 ± 1.6	NA
<b>PCWP, mmHg</b>	11 ± 1.6	NA

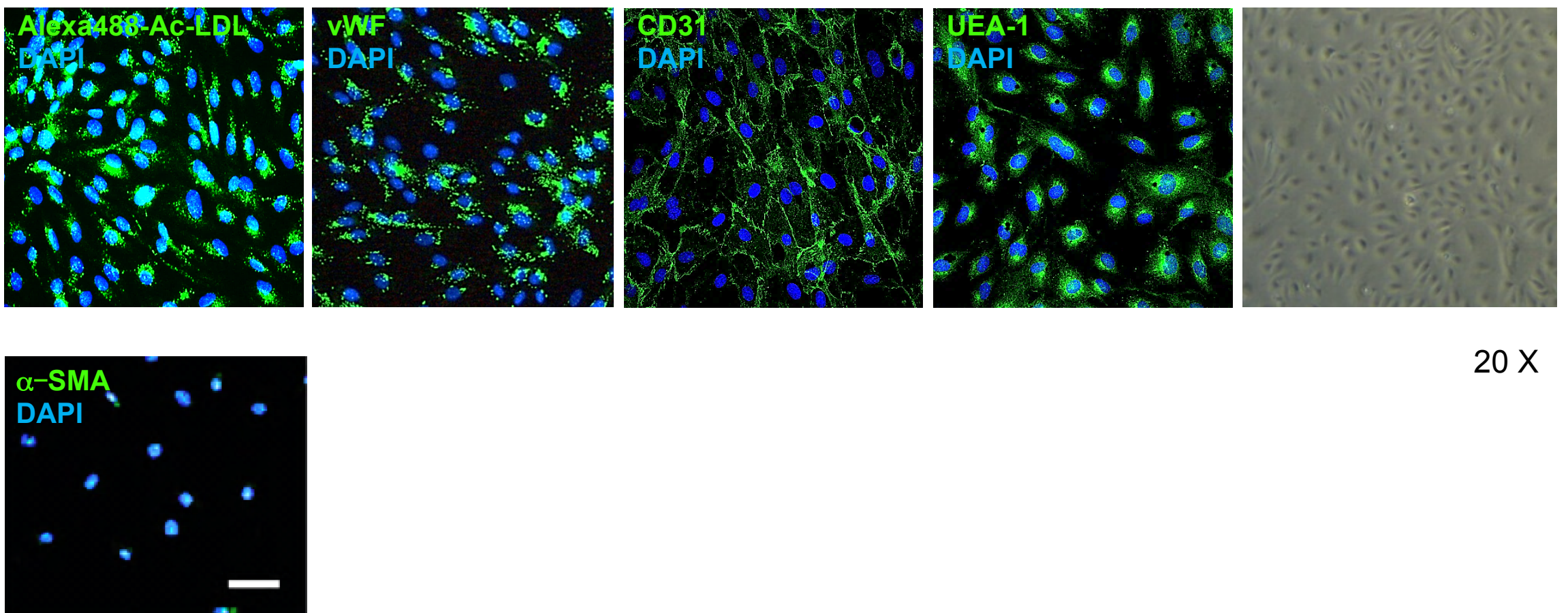
NYHA=New York Heart Association; mPAP=mean pulmonary artery pressure; CI=cardiac index; PVRi=pulmonary vascular resistance index; PCWP=pulmonary capillary wedge pressure; NA =not applicable

**Supplemental Table 2 – Characteristics Of Controls And Patients With Pulmonary Arterial Hypertension (PAH) For Determination of MIF and D-Dopachrome Tautomerase (DDT) Protein Levels:**

	<b>Controls</b> n=20	<b>iPAH</b> n=25	<b>hPAH</b> n=15
<b>Age, yrs</b>	38 ± 3	54 ± 3	47 ± 2
<b>Sex, MF (ratio)</b>	8/12 (0.67)	5/20 (0.25)	6/9 (0.67)
<b>NYHA functional class, n</b>			
class I	NA	3	1
class II	NA	16	8
class III	NA	6	6
class IV	NA	0	0
<b>6-MWD, m</b>	NA	465 ± 21	469 ± 13
<b>mPAP, mmHg</b>	NA	45 ± 3	49 ± 1.8
<b>CI, l/min/m<sup>2</sup></b>	NA	3.0 ± 0.2	2.1 ± 0.2
<b>PVR, Wood unit</b>	NA	6.4 ± 0.7	7.1 ± 0.6
<b>PcwP, mmHg</b>	NA	8 ± 0.6	8 ± 0.6
<b>RAP, Wood unit</b>	NA	5 ± 0.9	6 ± 0.8
<b>Specific PAH Therapy</b>			
- ERA	NA	11	0
- PDE-5i	NA	0	0
- ERA + PDE-5i	NA	8	6
- ERA + PGI <sub>2</sub>	NA	2	2
- PDE-5i + PGI <sub>2</sub>	NA	2	1
- ERA + PDE-5i + PGI <sub>2</sub>	NA	2	6
- No Treatment	NA	0	0

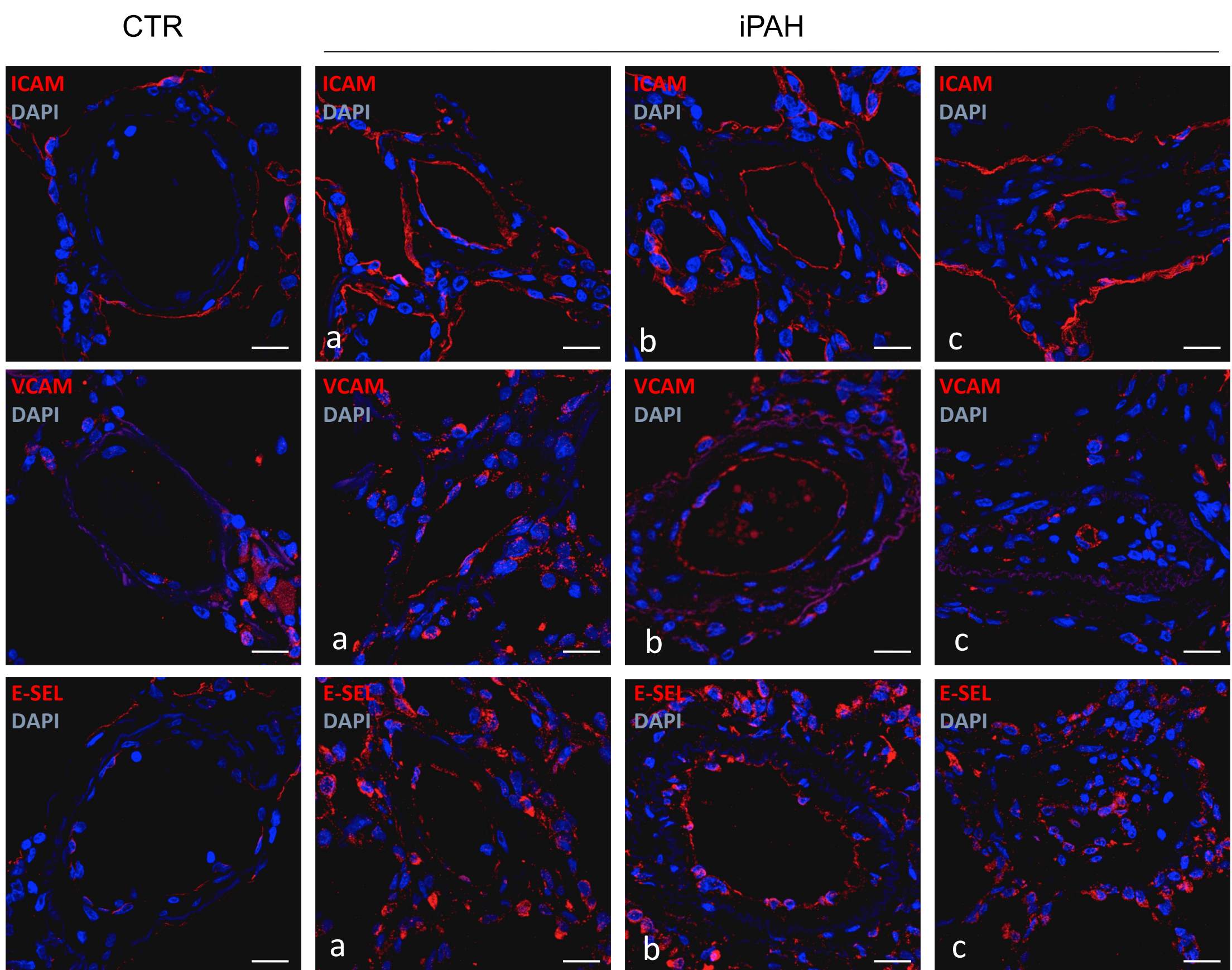
iPAH= idiopathic pulmonary arterial hypertension; hPAH= heritable pulmonary arterial hypertension; NYHA=New York Heart Association; 6-MWD=6 minute walk distance; mPAP=mean pulmonary artery pressure; CI=cardiac index; PVR= pulmonary vascular resistance; PcwP=pulmonary capillary wedge pressure; ERA=endothelin receptor antagonists; PDE-5i=Phosphodiesterase 5 inhibitors; PGI<sub>2</sub>: prostacyclin; NA = not applicable

### Supplemental Fig S1.

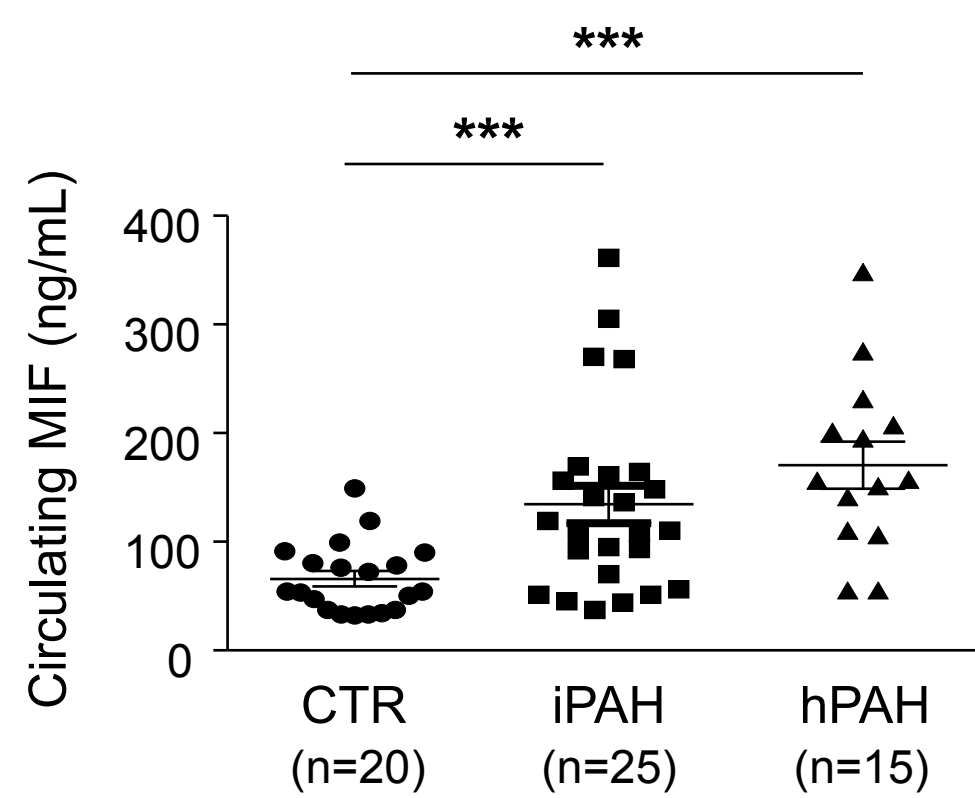


**Supplemental Fig S1.** Characterisation of human pulmonary endothelial cells (P-ECs) in primary cultures: The isolated P-ECs were strongly positive for acetylated low-density lipoprotein coupled to Alexa 488 (Alexa488-Ac-LDL), von Willebrand factor (vWF), CD31, and for Ulex europaeus agglutinin-1 (UEA-1) and negative for  $\alpha$ -smooth muscle actin ( $\alpha$ -SMA).

## Supplemental Fig S2.

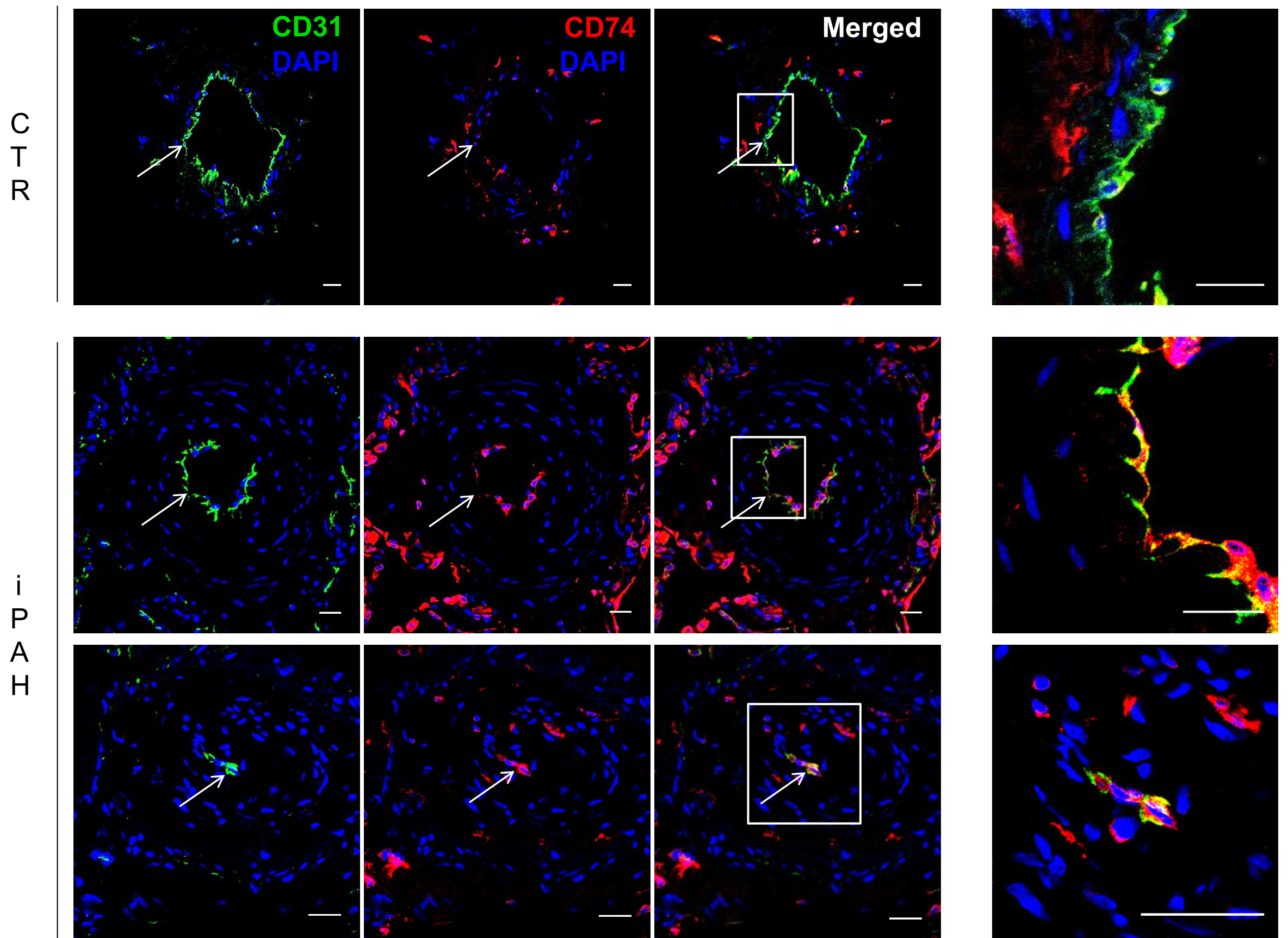


**Supplemental Fig S2.** Increased expressions of adhesion molecules in endothelium of pulmonary arteries in human idiopathic pulmonary arterial hypertension (iPAH) with various degrees of muscularization [non muscularized (a), midly muscularized (b), and muscularized (c)]. Representative images of intercellular adhesion molecule (ICAM)-1, vascular cell adhesion molecule (VCAM)-1, and E-selectin in pulmonary endothelium in lungs from control (CTR) subjects and patients with iPAH. Scale bar = 50  $\mu$ m in all sections.

**Supplemental Fig S3.**

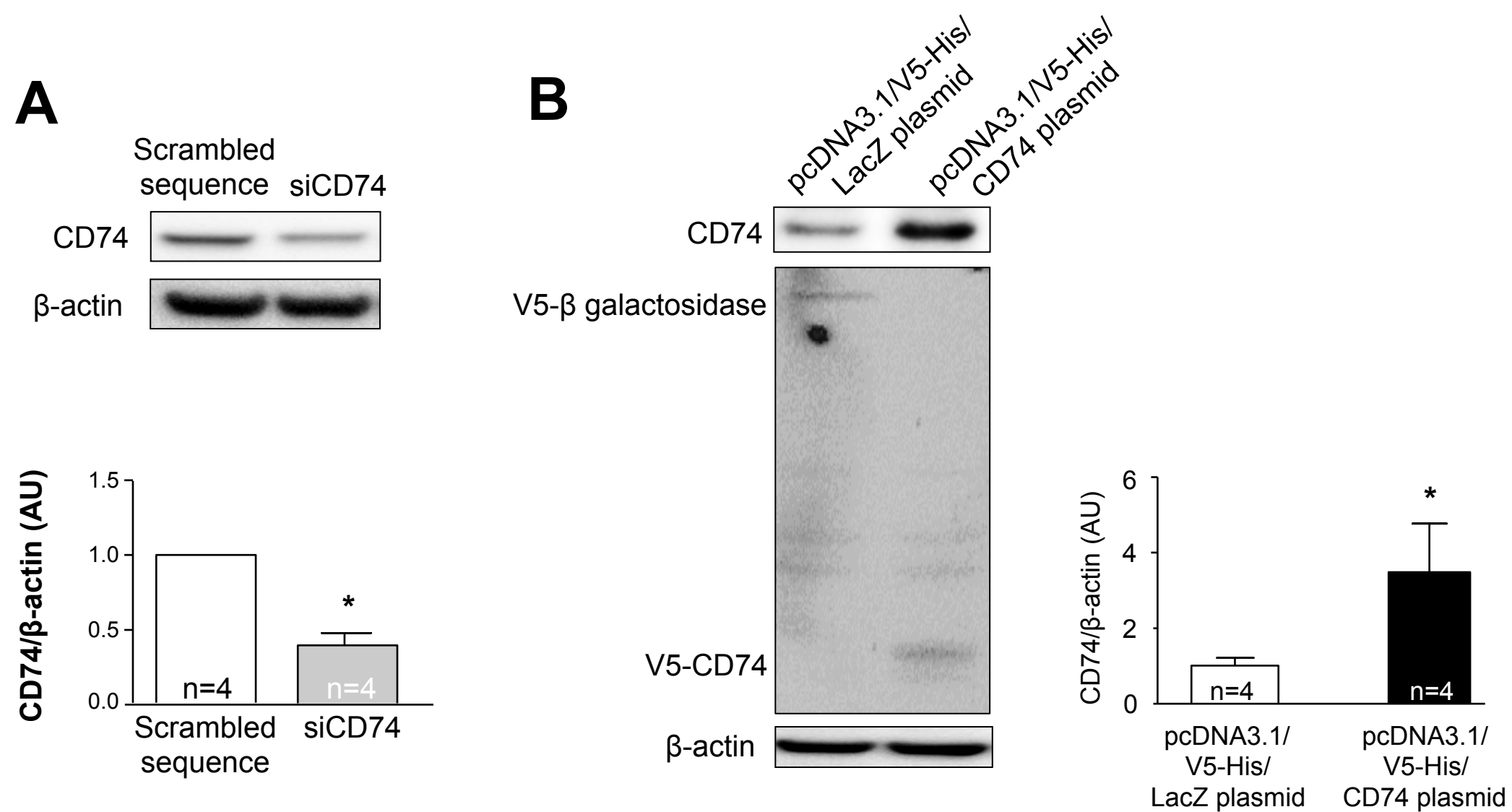
**Supplemental Fig S3.** Levels of circulating MIF protein in the serum of patients with idiopathic pulmonary arterial hypertension (iPAH), of patients with heritable (hPAH) carrying a BMP receptor 2 mutation and controls (CTR). \*\*\* p-value < 0.001 compared with CTR.

## Supplemental Fig S4.



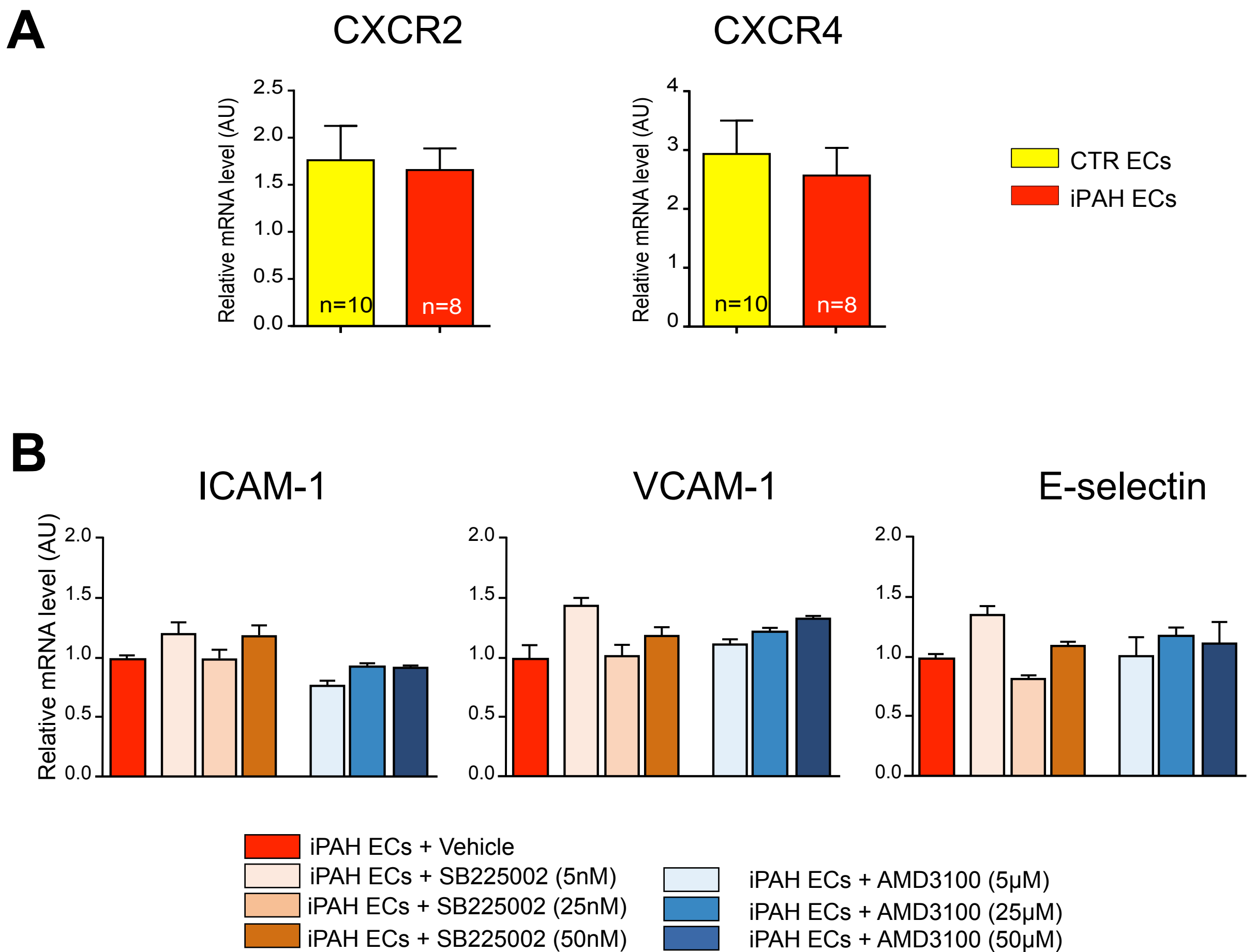
**Supplemental Fig S4.** Representative photomicrographs for CD74 immunostaining in distal pulmonary arteries in lung sections from controls (CTR) and idiopathic pulmonary arterial hypertension (iPAH) patients.

## Supplemental Fig S5.

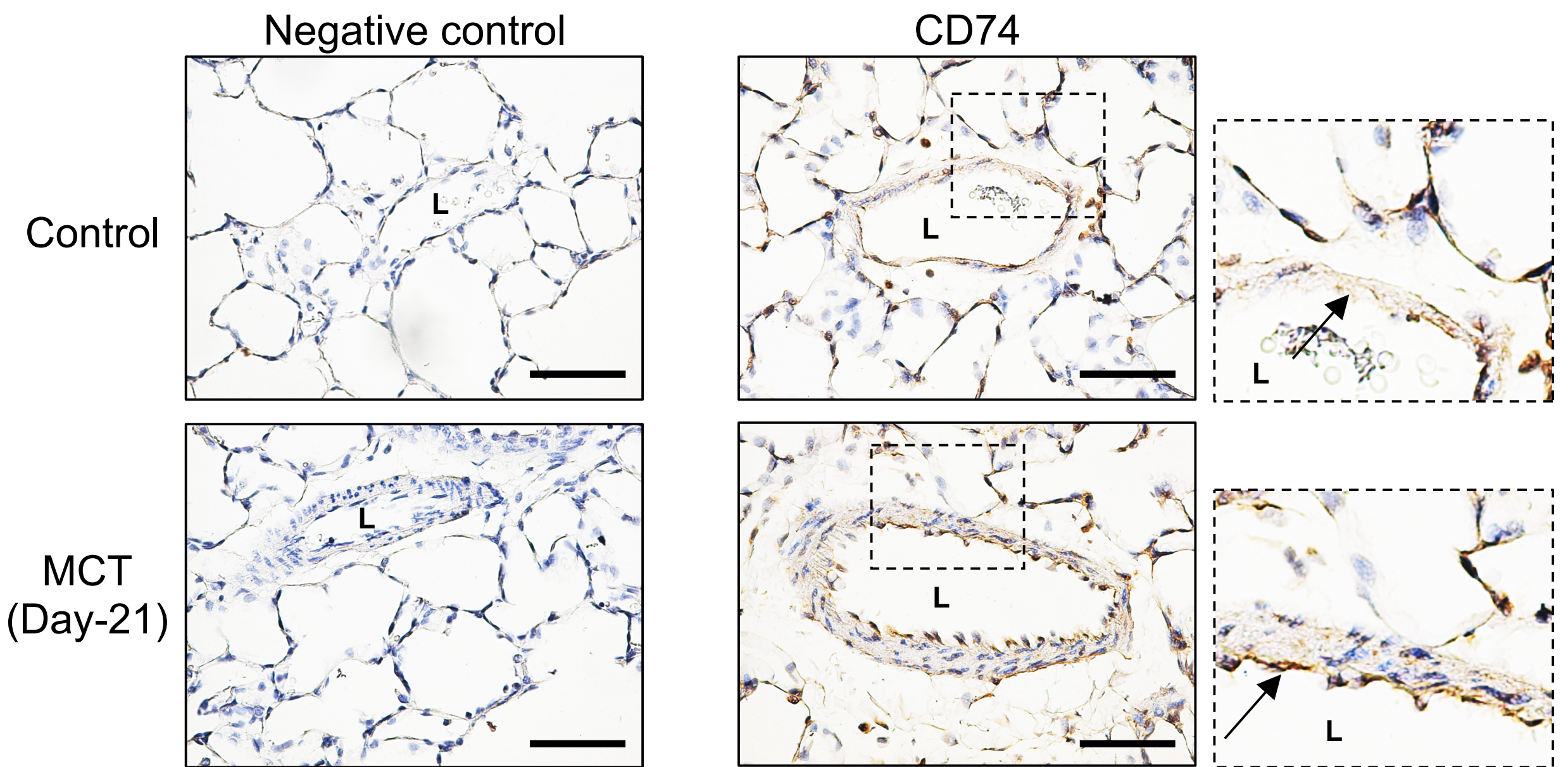


**Supplemental Fig S5.** Representative Western blots and quantification of the CD74/ $\beta$ -actin ratio in pulmonary endothelial cells (P-ECs) from control (CTR) patients transfected or not with scrambled sequence, or with siRNA against CD74, or with pcDNA3.1/V5-His/CD74 plasmid, or with pcDNA3.1/V5-His/LacZ plasmid. Values are means  $\pm$ SEM (n=4). \* p-value < 0.05 compared with CTR P-ECs transfected with scrambled sequence (siCTR) or pcDNA3.1/V5-His/LacZ plasmid.

## Supplemental Fig S6.

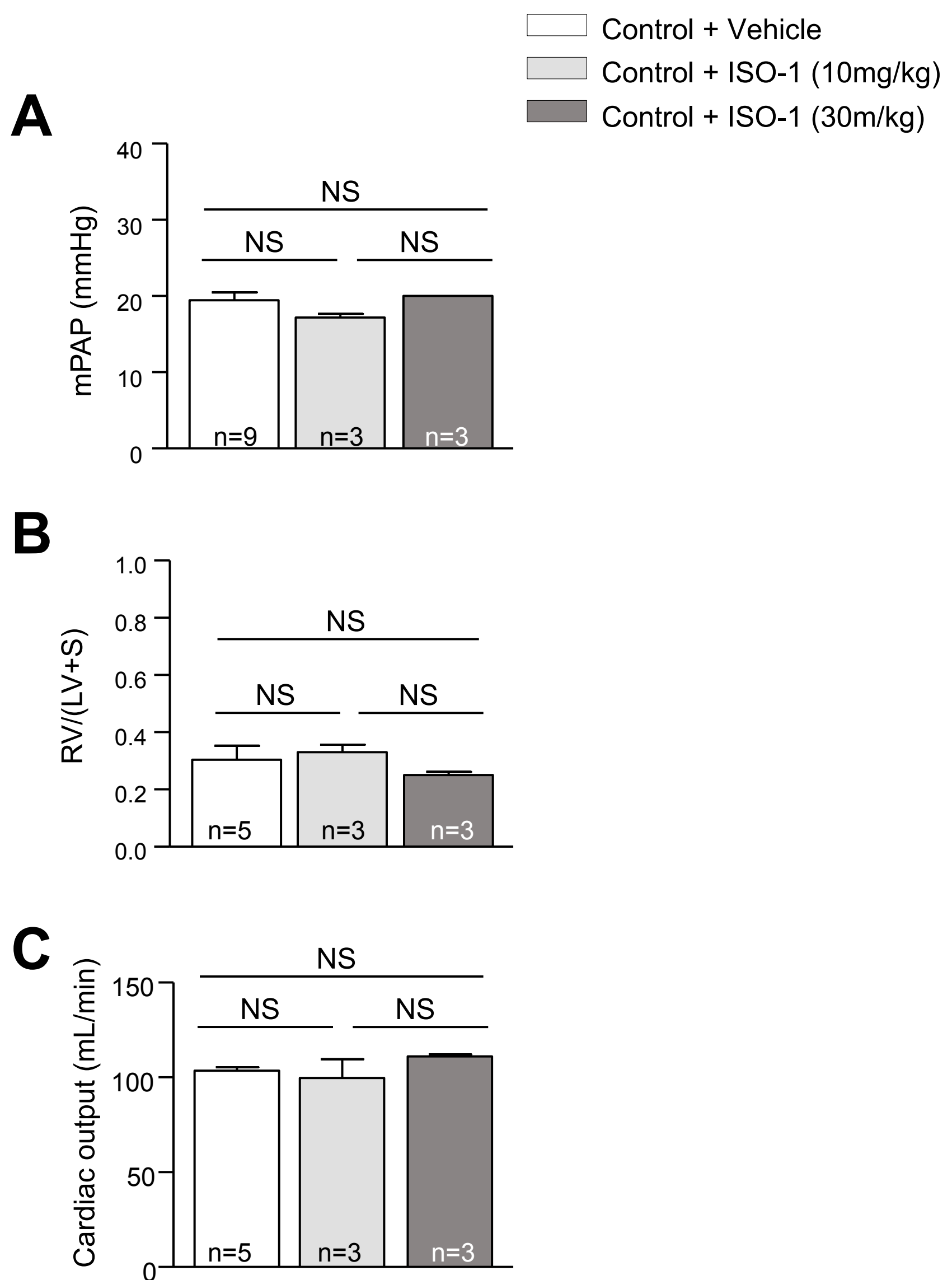


**Supplemental Fig S6.** Evaluation of the role of the CXCR2 and CXCR4 in the aberrant endothelial pro-inflammatory phenotype. **A:** Relative mRNA levels of CXCR2 and CXCR4 in primary early (<3) passage cultures of human pulmonary endothelial cells (P-ECs) established from lung tissue obtained from control (CTR) and idiopathic pulmonary arterial hypertension (iPAH) patients. **B:** Effects of pretreatments of iPAH ECs with the selective nonpeptide CXCR2 antagonist SB225002 (5, 25 and 50nM) or the CXCR4 blocking agents AMD3100 (5, 25 and 50 μM) for 24 h on the relative mRNA level of intercellular adhesion molecule (ICAM)-1, vascular cell adhesion molecule (VCAM)-1, and E-selectin.

**Supplemental Fig S7.**

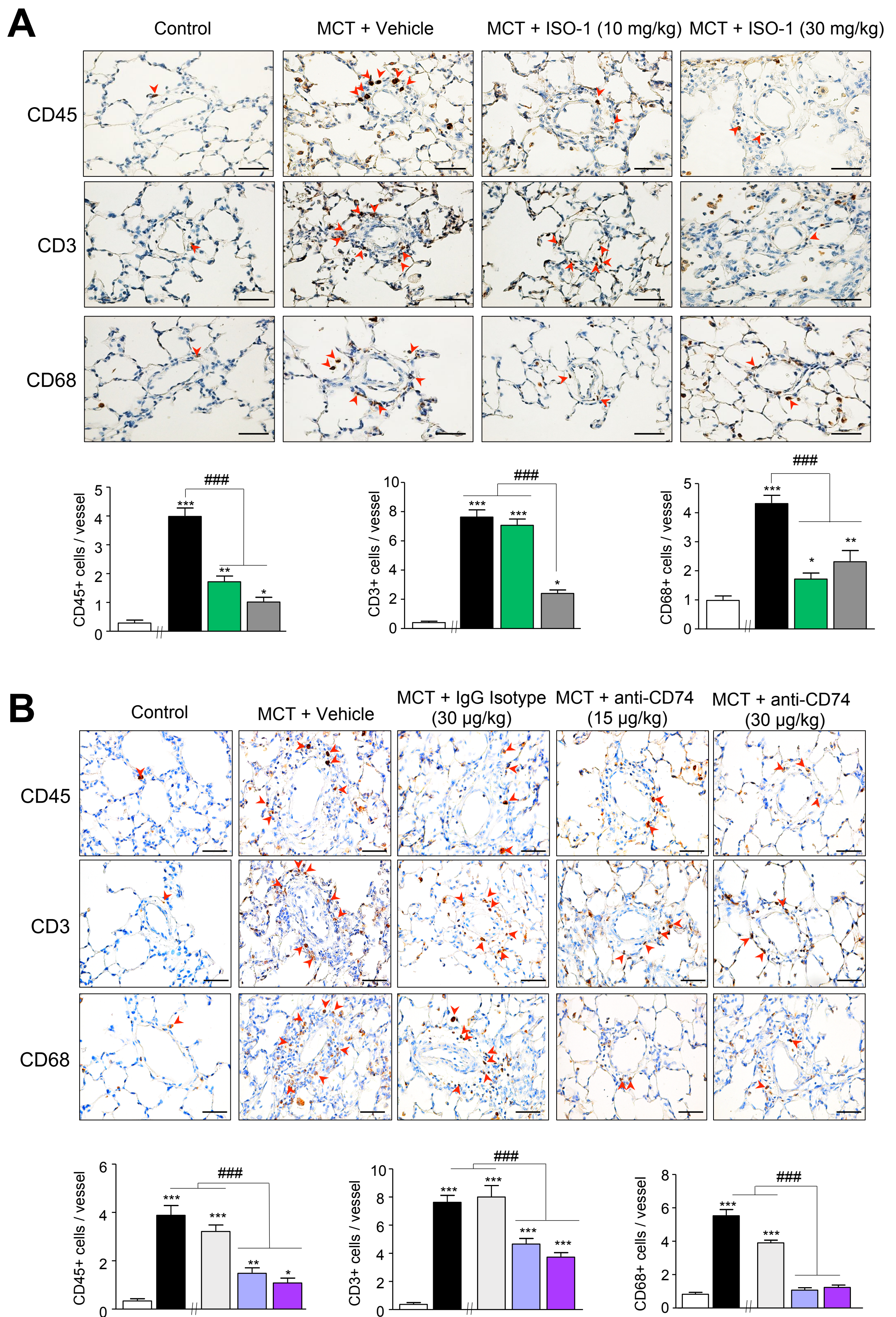
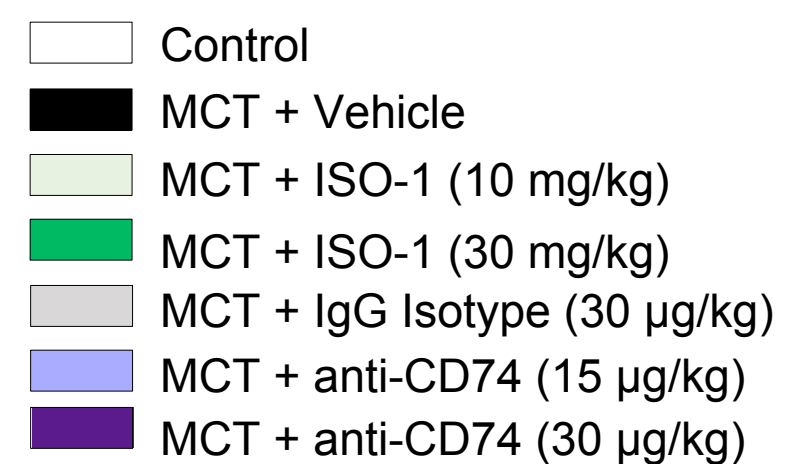
**Supplemental Fig S7.** Representative photomicrographs of CD74 immunostaining in distal pulmonary arteries in lung sections from control animals and monocrotaline (MCT)-injected rats. L= vessel lumen. Scale bar = 50  $\mu$ m in all sections.

### Supplemental Fig S8.



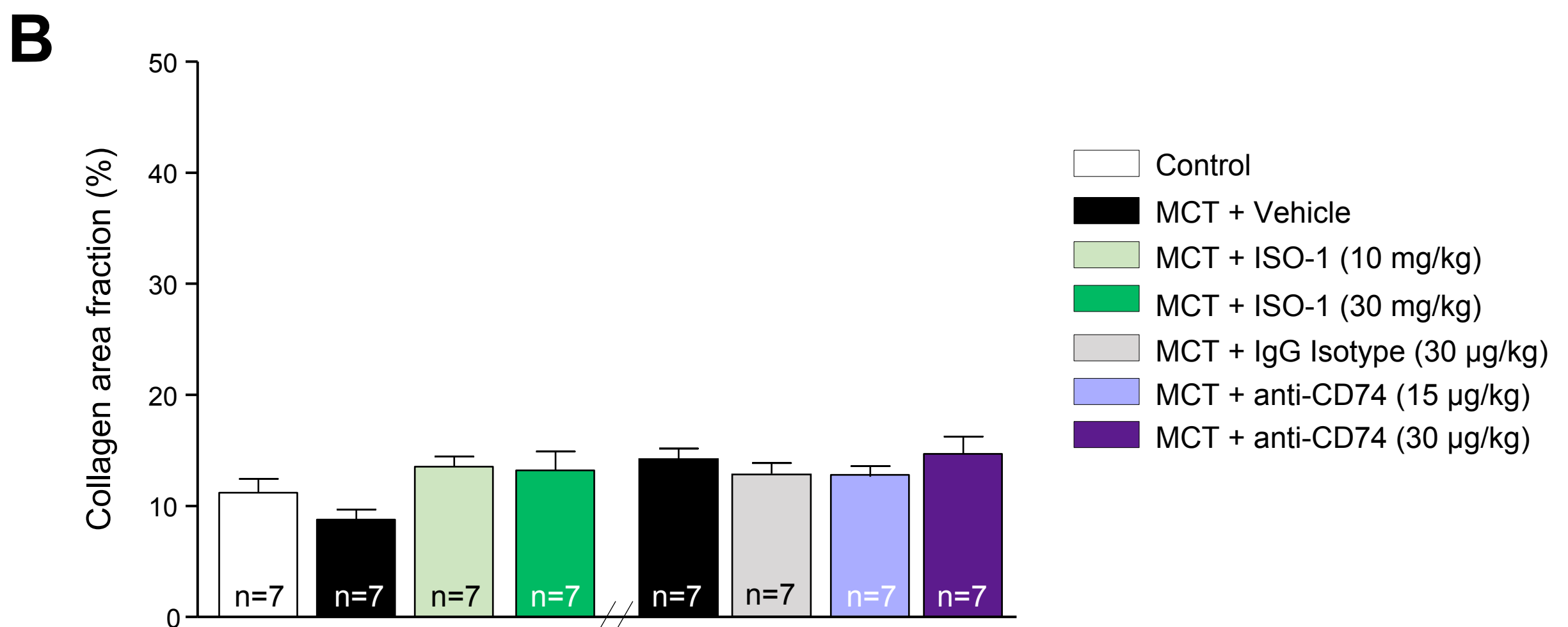
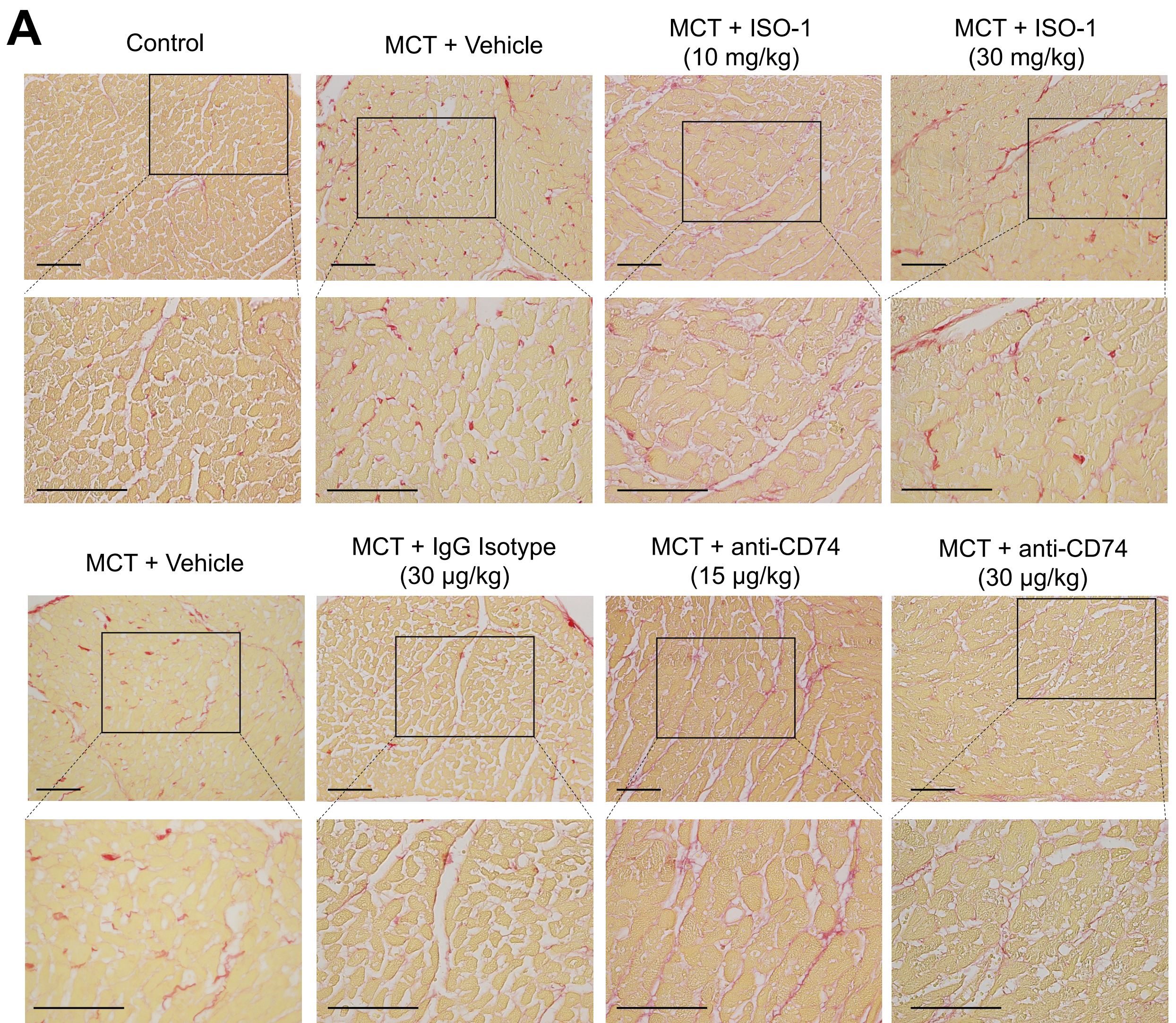
**Supplemental Fig S8.** Evaluation of the effect of ISO-1 treatments on the pulmonary hemodynamics in control rats. **A:** mean pulmonary arterial pressure (mPAP), **B:** right ventricular hypertrophy (Fulton index), **C:** cardiac output. NS= non significant.

## Supplemental Fig S9.



**Supplemental Fig S9.** Representative images and quantifications of immunostainings in rat lungs for CD45 (leukocyte common antigen), CD3 (T-lymphocytes), and CD68 (macrophages). Values are means  $\pm$ SEM (n=3-6). \* p-value < 0.05; \*\* p-value < 0.01; \*\*\* p-value < 0.001 compared with control rats; ### p-value < 0.001 compared with monocrotaline (MCT)-injected rats treated or not vehicle or IgG isotype.

## Supplemental Fig S10.



**Supplemental Fig S10.** Evaluation of cardiac fibrosis in left ventricle myocardium of rats treated or not with ISO-1, anti-IgG isotype, or anti-CD74 neutralizing antibodies. **A:** Representative images of picrosirius staining of tissue section of left ventricle myocardium of control and monocrotaline (MCT)-injected rats treated with ISO-1. **B:** Representative images of picrosirius staining of tissue section of left ventricle myocardium of control and MCT-injected rats treated with IgG isotype, or anti-CD74 neutralizing antibodies. **C:** Quantification of the collagen area fraction. Values are means $\pm$ SEM (n=7). Scale bar = 100µm in all section.